Sox genes represent a family related by the *Sry*-type high-mobility group (HMG) box, and function as transcription factors in various developmental processes through binding to a conserved core DNA sequence [16]. Twenty *Sox* genes have been identified in mouse and human, and are classified by their HMG box sequences into subgroups A–H [17, 18]. The expression pattern of each gene tends to be conserved in mouse and chicken. Among them, *Sox9* (group E) is known to act as a sex-determining gene. Mutations of human *SOX9* cause campomelic dysplasia, a severe skeletal malformation syndrome associated in most cases with XY sex reversal [19, 20], and ectopic expression of *Sox9* in XX mouse fetal gonads induces testis formation [21].

AMH plays an important role in inducing the regression of the Müllerian ducts in males, which normally give rise to the uterus, oviducts, upper vagina and fallopian tubes in females [22]. Analysis of mouse and human *Amh* gene regulation has uncovered several factors important for modulating *Amh* expression. For example, SF1 up-regulates *Amh* expression by cooperative interaction with WT1 [23], GATA-4 [24], SOX9 [25] and SOX8 [26]. Mice mutant for the SOX-binding site or the SF1-binding site in the *Amh* promoter revealed that SOX proteins are essential for *Amh* expression, while SF1 enhances the final expression level [27]. Oréal et al. [28] were the first to describe the chicken *Amh* promoter and showed that it has little overall homology with the mouse *Amh* promoter, but contains two putative SOX-binding sites and one SF1-binding site, suggesting that the mouse and chicken *Amh* promoters are similarly regulated. However, chicken *Sox9* is expressed too late to be a *cAmh* regulator [28, 29], but another SOX protein might substitute for SOX9 and, together with SF1, regulate *cAmh* expression.

Previously, we hypothesized that SOX8 might be a candidate transcription factor for regulating the chicken *Amh* gene [26, 30]. Mouse *Sox8* is expressed male specifically during gonad development. Its expression starts prior to the onset of *Amh* gene expression, and encodes a protein product that can up-regulate mouse *Amh* together with SF1 in vitro [26]. Group E Sox genes, consisting of Sox8, Sox9 and Sox10, show moderate levels of amino acid similarity and have similar genomic organization, suggesting that group E *Sox* genes may originate from one ancestral gene [31]. Although expression patterns of *Sox9* and *Sox10* overlap to a limited extent [32, 33], expression of *Sox8* overlaps substantially with expression of *Sox9* [31, 32] and to a lesser extent, *Sox10* [33, 31]. This fact suggests that there is some functional redundancy between SOX8 and SOX9, similar to that published for SOX1, SOX2 and SOX3 in lens formation [34], L-SOX5 and SOX6 in cartilage formation [35] and SOX7, SOX17 and SOX18 in vasculogenesis [36–38].

In this study, we analyzed the expression patterns of chicken *Sox8* in developing gonads during the sex-determining window. If *cSox8* contributes to *cAmh* gene expression, one would expect to find *cSox8* predominantly expressed in the embryonic testis and prior to the onset of *cAmh*. We found this not to be the case, suggesting that SOX8 is not responsible for sex-specific expression of *cAmh* in chicken. We also tested the expression patterns of several other *cSox* genes which are expressed in embryonic testis, and similarly found that they were not expressed male specifically.

Materials and methods

Chicken embryos. Fertilized chicken eggs were obtained from local suppliers (Ingham, Brisbane, Australia and Saitama Experimental Animal Supply, Saitama, Japan) and maintained at 18 °C until use. Eggs were transferred to an incubator at 37.5 °C and allowed to develop for 5, 6 or 7 days. Staging was confirmed at dissection according to Hamburger and Hamilton [39]. The entire urogenital ridge of each embryo was explanted for whole-mount *in situ* hybridization. Sexing was performed by PCR as described elsewhere [40] using genomic DNA purified from a hind limb of each embryo.

Amplification of HMG box sequences. Total RNA was isolated from left and right gonads of day 6 male embryos by standard methods [41]. RNA (0.5 μg) was then treated with DNaseI and first-strand cDNA was synthesized using M-MLV reverse transcriptase (Invitrogen) according to the manufacturer's protocol. For amplification of the HMG box, the PCR reaction was carried out in a solution containing 1 x NH_4 buffer (Bioline), 100 M $MgCl_2$, 100 μM dNTPs, 0.4 μM primers and 0.5 unit Biotaq DNA polymerase (Bioline) with 4.5 min denaturation at 95 °C followed by 40 cycles of amplification at 95 °C for 30 s and 57 °C for 30 s. The PCR product was cloned into pGEM-T Easy (Promega). Sequencing was performed using the BigDye Terminator v3.1 Cycle Sequencing Kit (Applied Biosystems) and M13 reverse primer, and electrophoresis was carried out by the Australian Genome Research Facility, Brisbane, Australia. Primer sequences used were as follows; G7A1: 5'-AGC G(A/G)C CCA TGA ACG C(A/C/G/T)T T-3' and G7B1: 5'-CGC (C/T)GG TA(C/T) TT(A/G) TA(A/G) TC(A/C) GGG T-3'. The PCR reaction was also carried out using genomic DNA as a template.

RT-PCR of *Sox* genes, *Amh* and *Actin*. The left and right gonads of staged, sexed embryos were pooled (ten and five embryos of each sex for day 6 and day 7, respectively) to isolate total RNA using the RNeasy Mini kit (Qiagen) with the optional on-column DNase digestion with the RNase-free DNase set. The first-strand cDNA was synthesized from 1 μg of total RNA using Power-

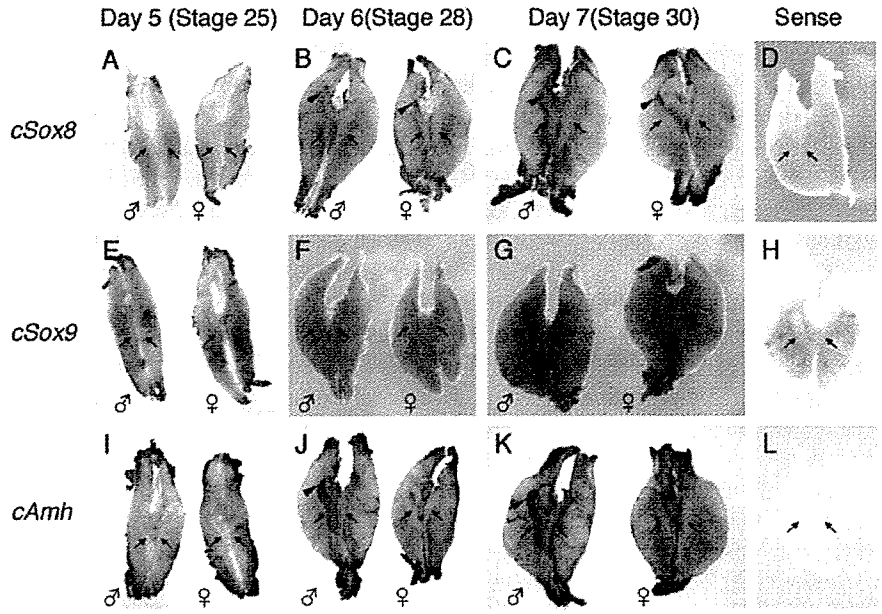

Figure 1. Whole-mount *in situ* hybridization of *cSox8*, *cSox9* and *cAmh* in the chicken embryonic gonad/mesonephros. In each panel, male (♂) and female (♀) gonad/mesonephros are left and right, respectively. Probes used are shown at the left of each panel. The samples in A–C, E–G and I–K were hybridized with antisense probe. In D and L a day 6 sample hybridized with sense probe. In H a day 7 sample was hybridized with sense probe. Developmental stages (days and Hamburger-Hamilton stage) of gonad/mesonephros are labeled above. Arrow shows the position of gonad. Arrowheads point to regions of positive staining.

Script reverse transcriptase (Clontech) and oligodT. PCR amplification was carried out using the QuantiTect SYBR Green PCR kit (Qiagen) with uracil-N-glycosylase and the 7900HT Sequence Detection System (Applied Biosystems). Samples were incubated at 50 °C for 2 min, then 95 °C for 15 min, followed by 40 cycles of amplification at 94 °C for 30 s, 54.2 °C for 1 min and 72 °C for 1 min. For the amplification of *cSox8* and *cSox9*, 85.4 °C for 15sec was added after each 72 °C step of each amplification cycle. Primer sequences used were as follows; cSox3-1: 5'-GCACCAGCACTACCAGAG-3' and cSox3-2: 5'-CGA ATG CGG ACA CGA ACC) for *cSox3* [29], cSox4F: 5'-TCG GGG GAT TGG CTG GAG TC-3' and cSox4R: 5'- CTC AGC CGA TCC TCG TTT CC-3' for *cSox4*, cSox8RTF : 5'-CTA CAA GGC TGA CAG CGG GC-3' and cSox8RTR: 5'-AGG CCG GGC TCT TGT GAG TC-3' for *cSox8*, cSox9F: 5'-CCC CAA CGC CAT CTT CAA-3' and cSox9R: 5'-CTG CTG ATG CCG TAG GTA-3' for *cSox9*, cSox11F2: 5'-AAG CAG GAG GCG GAC GAC GA-3' and cSox11R2: 5'-CGC CCC GCA CCT CCT CGT AG-3' for *cSox11*, cAmh-1: 5'-GTG GAT GTG GCT CCC TAC CC-3' and cAmh-2: 5'-GCA GCA CCG AGG GCT CCT CC-3' for *cAmh* [29] and Actin-1: 5'-TGG ATG ATG ATA TTG CTG C-3' and Actin-2: 5'-ATC TTC TCC ATA TCA TCC C-3' [29] for *Actin*. To calculate the relative amount of gene expression levels, the $\Delta\Delta C_T$ method was used. Three independent pooled samples were analyzed. Maximum average values were set as 100%.

For the RT-PCR amplification of *cSox12* and *cSox14*, the same cDNA for the real-time RT-PCR was used. The PCR reaction was carried out in the same solution as HMG box amplification with 4.5 min denaturation at 95 °C followed by 40 cycles of amplification at 95 °C for 30 s and 50 °C for 30 s. Primer sequences used were as follows; cSox12F: 5'-AGA TCT CCA AGC GCC TGG GTC G-3' and cSox12R: 5'-GGT AGT CGG CCA TGT GCT TG-3' for *cSox12*, cSox14F: 5'-GAG GTT CCT CAC ACC TTG GC-3' and cSox14R: 5'-ACA CGG AGG AAT CCC AGT CC-3' for *cSox14*.

Probes. The previously reported *cAmh* probe [9] was obtained by RT-PCR amplification of an 821-bp fragment, using primers cAMHRTF (5'-ACG GTG CGC GCC CAC TGG CAG G-3') and cAMHRTR (5'-ACG TCG TGA CCT GCA AGC CCT C-3') and RNA prepared from 5.5-day-old whole embryo. The *cSox8* probe was cloned by PCR using primers chSox8C2F (5'-CTG CAG AGC TCC AAC TAC TAC A-3') and chSox8C2R (5'-GAG CTC TGT CCT TTT GGA GAG T-3') and chicken genomic DNA as the template. The fragment corresponds to nucleotides 1228–1589 of the *cSox8* mRNA sequence (accession No. AF228664). PCR products of *cAmh* and *cSox8* were cloned into the pGEM-T Easy vector. The *cSox9* probe was reported previously by Kent et al. [11]. The *cSox11* fragment was cloned by SacI digestion of *cSox11* cDNA and subsequent insertion into pBluescriptII KS vector. The fragment corresponds to nucleotides 667–967 of the *cSox11* mRNA sequence (accession No. AB012237). The *cSox4* probe was obtained by KspI digestion of *cSox4* cDNA and subsequent insertion into pBluescriptII KS vector. The fragment corresponds to nucleotides 576–965 of the chicken *Sox4* mRNA sequence (accession No. AY493693).

***In situ* hybridization.** Sense and antisense digoxygenin-labeled RNA probes were generated by *in vitro* transcrip-

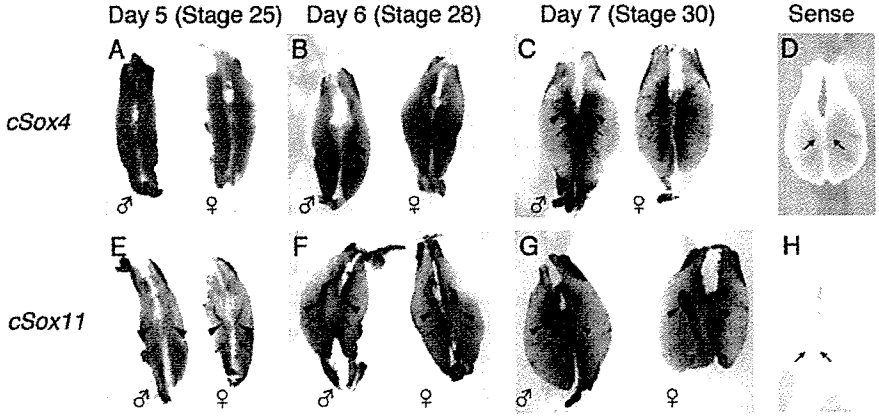

Figure 2. Whole-mount *in situ* hybridization of *cSox4* and *cSox11* in the chicken embryonic gonad/mesonephros. In each panel, male (♂) and female (♀) gonad/mesonephros are left and right, respectively. Probes used are shown at the left of each panel. A–C and E–G were hybridized with antisense probe. D and H show day 6 samples hybridized with sense probe. Developmental stages (days and Hamburger-Hamilton stage) of gonad/mesonephros are labeled above. Arrow shows the position of gonad. Arrowheads point to regions of staining.

tion. Whole mount *in situ* hybridization was performed as described using the maleic acid buffer (MABT) method [42]. Experiments were carried out at least twice for each probe, with similar results.

Results and discussion

To compare the temporospatial expression of *cSox8* and *cAmh* in embryonic gonads, we employed whole-mount *in situ* hybridization analysis using female and male gonad/mesonephros complexes isolated from day 5, 6 and 7 chicken embryos (Hamburger and Hamilton stages 25, 28 and 30, respectively [39]). These stages cover the temporal window at which sexual dimorphism in the gonad first becomes apparent [43]. In addition to providing spatial information relating to gene expression, whole-mount *in situ* hybridization is commonly used as a semiquantitative guide to gene expression levels between different tissues hybridized with the same probe and incubated under the same conditions, as in the experiments described below.

As expected, *cAmh* was expressed at higher levels in male than in female gonads at day 6 and 7 (fig. 1J, K). Expression levels in the right male gonads were higher than in the left, possibly reflecting the asymmetric development of avian genital ridges [43]. We did not observe expression of *cAmh* at day 5 (fig. 1I), even though Oréal et al. [28] reported that *cAmh* is expressed weakly and at similar levels in male and female gonads at day 5 by section *in situ* hybridization. This may reflect lower sensitivity of our whole mount *in situ* hybridization method.

Previous workers have reported that male-specific high-level expression of *cSox9* is preceded by expression of *cAmh* in the chick [28, 29]. We analyzed the temporal expression of *cSox9* in chicken embryos. No signal was observed in male or female gonads at day 5 or day 6 (fig. 1E, F). High levels of *cSox9* expression were observed in day 7 male gonads, while no signal was observed in the day 7 female (fig. 1G). This compares to the results of Oréal et al. [28] who described very faint expression of *cSox9* in day 6 gonads by *in situ* hybridization using sections. Our data demonstrate high levels of *cAmh* expression in day 6 male gonad, preceding the high levels of *cSox9* expression first detected in day 7 male gonad. They suggest that SOX9 is not responsible for the male-specific up-regulation of *cAmh*, but may play a role in the maintenance and/or amplification of *cAmh* expression in the male gonads once transcription is initiated. Our results support the previous observation that the male-specific high levels of *cAmh* expression precede testicular *cSox9* expression [28, 29].

We next examined expression of *Sox8*. At day 5, no *cSox8* expression was observed (fig. 1A). At day 6 and 7, *cSox8* expression was observed at the anterior tip of both male and female right gonads at similar levels (fig. 1B, C). This expression profile is different from that of *cAmh*, both in spatial distribution of transcripts and degree of sex specificity, suggesting that SOX8 could not be responsible for sex-specific up-regulation of *cAmh* in chicken.

The expression patterns of mouse and chicken *Sox8* imply that the functions of SOX8 are conserved in most but not all tissues between the two species. For example, *Sox8* is expressed in brain, skeletal muscle, eye, somite, dermomyotome, limb, digits, gut, spinal cord and dorsal root ganglia in both species [30, 31, 44]. However, some differences are evident in embryonic heart and gonad: in chicken, *cSox8* is expressed in the embryonic heart, testis and ovary, whereas in mouse, *Sox8* expression occurs predominantly in the embryonic testis, but not in the ovary or heart [31, 44]. Given these observations, SOX8 may contribute to the male-specific activation of *Amh* expression during gonadgenesis in mice but not chicken.

In mouse, only two SOX proteins, SOX8 and SOX9, have been identified as regulators of *Amh* expression in the embryonic gonad [26]. Based on our data, and previous studies [28, 29], neither SOX8 nor SOX9 can be responsible for the onset of high levels of *cAmh* expression

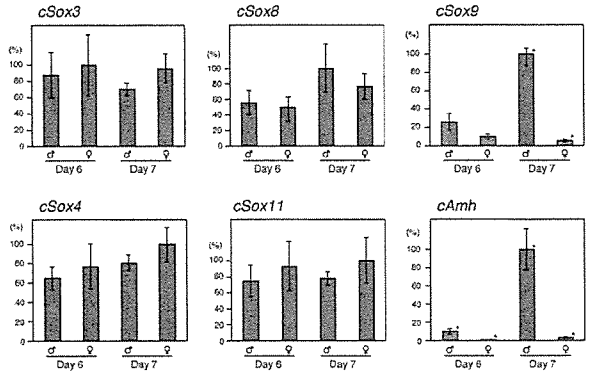

Figure 3. Quantitative, real-time RT-PCR analysis of *Sox* and *Amh* gene expression. Averages of three independent trials are shown as bars, with SEs shown as lines. Values marked with * were significantly different between males (♂) and females (♀) ($p = 0.0017$, 0.0047 and 0.012 for cSox9 at day 7, cAmh at day 6 and 7, respectively, using a two-sample equal variance t-test). Others were not significantly different between males and females ($p = 0.81$, 0.24, 0.74, 0.52, 0.17, 0.67, 0.38, 0.64, 0.49 for *cSox3* at day 6 and 7, *cSox8* at day 6 and 7, *cSox9* at day 6, *cSox4* at day 6 and 7, and *cSox11* at day 6 and 7, respectively).

in chicken, even though two SOX-binding sites are predicted in the *cAmh* promoter region. These observations prompted us to search for other *Sox* genes expressed in chicken male gonads that could be considered as candidate regulators of *Amh* expression. We conducted the analysis at day 6, since at this stage *cAmh* is expressed at high levels in male gonads while *cSox9* is either not expressed or expressed at a very low level.

We utilized degenerate RT-PCR on purified day 6 male gonad RNA using generic *Sry*-type HMG box primers to generate fragments for cloning into a plasmid vector. Twenty independent clones were sequenced, revealing that 12 clones were *cSox4* [45], 7 were *cSox11* [46] and 1 was *cSox9* [47].

One possible explanation for these results is that the degenerate primers used show a bias for amplification of *cSox4* and *cSox11* templates. To examine this possibility, we used the same degenerate primers to amplify *Sox* fragments from genomic DNA, in which all intronless *Sox* genes (Sox1, -2, -3, -4, -11, -12, -14, -21) capable of amplification by the primers are represented in equal proportions. Among ten clones amplified, none was *cSox4* or *cSox11*. Thus, primer bias does not explain our data relating to *cSox4* and *cSox11* expression in developing chicken gonads.

cSox4 and *cSox11* are expressed in male gonads at day 6, prompting us to examine the expression profiles of each in male and female gonads through the sex determination window. If both or either is expressed preferentially in male gonads, they could be considered a candidate for regulation of the *cAmh* gene. To evaluate the expression patterns of *cSox4* and *cSox11* in embryonic gonads, we employed whole-mount *in situ* hybridization analysis at the same stages previously used to profile *cSox8*, *cSox9* and *cAmh* expression. *cSox4* and *cSox11* signals were detected at similar levels in male and female gonads at all stages examined (fig. 2) suggesting that neither of them plays a role in sex-specific regulation of *Amh*.

The identification of *Sox* genes that are expressed in chicken embryonic gonads at day 5, 6 and 7 was previously attempted by McBride et al. [6]. Using RT-PCR amplification of the conserved *Sry*-type HMG box domain from RNA samples prepared from testes with mesonephroi attached, they found expression of *cSox3*, *cSox4*, *cSox9*, *cSox11*, *cSox12* and *cSox14*. Our data confirm that *cSox4*, *cSox9* and *cSox11* are indeed expressed, as is cSox3 (see below); however; we amplified the HMG box from day 6 gonad only, and this difference along with the differences in PCR primers, may explain the discrepancies in the data for *cSox12* and *cSox14*. Moreover, day 6 male gonad expresses *cSox4* and *cSox11* transcripts so abundantly that RT-PCR cloning is difficult for *Sox* genes expressed at low levels.

To examine the levels of gene expression quantitatively, we utilized RT-PCR and real-time RT-PCR analyses using RNAs isolated from pooled, sexed embryonic gonads at days 6 and 7 (fig. 3). As expected, *cAmh* and *cSox9* were expressed at different levels between males and females at day 7. At day 6, the expression levels of *cAmh* were statistically different between males and females ($p < 0.005$) while the expression levels of *cSox9* were not ($p > 0.1$). However, *cSox3*, *cSox4*, *cSox8* and *cSox11* were expressed at similar levels between males and females at days 6 and 7, suggesting that none of these *Sox* genes is responsible for the male-specific up-regulation of *cAmh* expression.

We were unable to amplify *cSox12* and *cSox14* sequences by RT-PCR from chicken embryonic gonads. As a positive control, chicken genomic DNA was included as template. Signals were observed at expected size of 108 bp for *cSox12* and 331 bp for *cSox14* only from genome template, but not from gonad RNA samples, showing that neither gene is expressed in embryonic gonads at day 6 and day 7 (data not shown).

Previous studies have eliminated *cSox3* as a candidate for male-specific up-regulation of *Amh* expression because *cSox3* is expressed at similar levels in the male and female gonads at the sex-determining window [28, 29]. Our present data support this conclusion. We rule out *cSox8* because it is expressed in a different spatial pattern to *Amh*, and *cSox12* and *-14* because they are not expressed in gonads at sex-determining stages at all. We exclude *cSox4* and *cSox11* also, on the basis of equivalent expression levels between male and female. It is formally possible that *cSox4* and *cSox11* might be expressed in Sertoli cells in the male (the site of *Amh* expression) and in another cell lineage in females, in which *Amh* is

not expressed, but we consider this unlikely, especially considering that all genes found to be involved in sex-specific development of the gonads to date show a sexually dimorphic pattern of gene expression in fetal gonads when examined by whole-mount *in situ* hybridization. However, one still cannot exclude the possibility of SOX protein-mediated regulation of *cAmh* gene expression, and further extensive cloning of *cSox* genes may be necessary to discover a *Sox* gene expressed predominantly in chicken embryonic testis.

Alternatively, we have to consider that sex-specific *Amh* up-regulation is not mediated by SOX proteins in birds. Even though the putative SF1-binding site, like the two SOX-binding site in the *Amh* promoter, is conserved between mouse and chicken [28], and *cSf1* is co-expressed with *cAmh* at day 7 of chicken embryonic testis [15], the expression profiles of mouse and chicken *Sf1* show major differences. Before testis cord formation, *Sf1* is expressed at similar levels in males and females in both species, while subsequently, chicken *Sf1* expression is maintained in the testis, but is up-regulated in the ovary [12, 15, 29]. The opposite expression pattern is reported for mouse *Sf1* [reviewed in ref. 48]. This difference could be explained by the possibility that *SF1* functions in more steroidogenically active tissue (testis in mammals and ovary in birds), or that *Sf1* may not be associated with testis formation in birds [12]. Either way, the expression profile of *cSf1*, like that of *cSox9* [28] and *cSox8* (this study), suggests that it is not responsible for male-specific up-regulation of *cAmh* expression during chicken gonad genesis. Since both SF1 and SOX proteins are required for normal levels of *Amh* expression during sex determination in mouse [27], this may imply that there is a different mechanism of *cAmh* regulation in chicken compared with mouse, and that SOX protein is not a causative factor for sex-specific expression of *cAmh*.

Gonadal expression of *Sox8*, which has an evolutionarily conserved coding protein among vertebrates, has been studied in mouse, chicken and red-eared slider turtle [31, 49]. *Sox8* is expressed in the developing testes of all three species, implying a functional significance, but in chicken and turtle, *Sox8* is also expressed in the ovary. So far, up-regulation of mouse *Amh* is the only known molecular function for the SOX8 protein [26]. If this function is conserved among vertebrates, chicken SOX8 may have a protein partner which is expressed in males to activate or in females to suppress *cAmh*. Some genes are expressed sex specifically during gonadal differentiation in the mouse, including *Sf1* [13], *Wt1* [50], *Gata4* [14], *Lhx9* [51], *Wnt-4* [52] and *Dax1* [53]. However, chicken homologues of these genes are not candidates because they are expressed in both developing testis and ovary while *cAmh* is differentially expressed [15, 29]. *Dmrt1* is expressed only in developing testis in mouse, while chicken *Dmrt1* is expressed in both developing gonads with higher levels in testis, suggesting that it is not such a factor [15, 54]. The identification of a chicken SOX8-binding partner may clarify this possibility. Finally, further analysis of the *cAmh* promoter may reveal whether SOX proteins play a role in its up-regulation, and whether similarities exist in the mechanisms that regulate *Amh* expression in birds and mammals.

Acknowledgements. We thank M. Hargrave, K. Loffler and J. Bowles and members of the Koopman laboratory for technical advice and constructive criticism, and D. Wilhelm and F. Martinson for critical reading of this manuscript. P. K. is a Professorial Research Fellow of the Australian Research Council.

1 Gubbay J., Collignon J., Koopman P., Capel B., Economou A., Münsterberg A. et al. (1990) A gene mapping to the sex-determining region of the mouse Y chromosome is a member of a novel family of embryonically expressed genes. Nature **346:** 245–250
2 Sinclair A. H., Berta P., Palmer M. S., Hawkins J. R., Griffiths B. L., Smith M. J. et al. (1990) A gene from the human sex-determining region encodes a protein with homology to a conserved DNA-binding motif. Nature **346:** 240–244
3 Koopman P., Gubbay J., Vivian N., Goodfellow P. and Lovell-Badge R. (1991) Male development of chromosomally female mice transgenic for Sry. Nature **351:** 117–121
4 Coriat A.-M., Muller U., Harry J. L., Uwanogho D. and Sharpe P. T. (1993) PCR amplification of SRY-related gene sequences reveals evolutionary conservation of SRY-box Motif. PCR Methods Appl. **2:** 218–222
5 Griffiths R. (1991) The isolation of conserved DNA sequences related to the human sex determing region Y gene from the lesser black-backed gull (Larus fuscus). Proc. R. Soc. Lond. B. **224:** 123–128
6 McBride D., Sang H. and Clinton M. (1997) Expression of Sry-related genes in the developing genital ridge/mesonephros of the chick embryo. J. Reprod. Fertil. **109:** 59–63
7 Tiersch T. R., Mitchell M. J. and Wachtel S. S. (1991) Studies on the phylogenetic conservation of the SRY gene. Hum. Genet. **87:** 571–573
8 Clinton M. (1998) Sex determination and gonadal development: a bird's eye view. J. Exp. Zool. **281:** 457–465
9 Carré-Eusèbe D., Clemente N. di, Rey R., Pieau C., Vigier B., Josso N. et al. (1996) Cloning and expression of the chick anti-Müllerian hormone gene. J. Biol. Chem. **271:** 4798–4804
10 Morais da Silva S., Hacker A., Harley V., Goodfellow P., Swain A. and Lovell-Badge R. (1996) Sox9 expression during gonadal development implies a conserved role for the gene in testis differentiation in mammals and birds. Nat. Genet. **14:** 62–68
11 Kent J., Wheatley S. C., Andrews J. E., Sinclair A. H. and Koopman P. (1996) A male-specific role for SOX9 in vertebrate sex determination. Development **122:** 2813–2822
12 Smith C. A., Smith M. J. and Sinclair A. H. (1999b) Expression of chicken steroidogenic factor-1 during gonadal sex differentiation. Gen. Comp. Endocrinol. **113:** 187–196
13 Ikeda Y., Shen W. H., Ingraham H. A. and Parker K. L. (1994) Developmental expression of mouse steroidogenic factor-1, an essential regulator of the steroid hydroxylases. Mol. Endocrinol. **8:** 654–662
14 Viger R. S., Mertineit C., Trasler J. M. and Nemer M. (1998) Transcription factor GATA-4 is expressed in a sexually dimorphic pattern during mouse gonadal development and is a potent activator of the Müllerian inhibiting substance promoter. Development **125:** 2665–2675
15 Oréal E., Mazaud S., Picard J.-Y., Magre S. and Carré-Eusèbe D. (2002) Different patterns of anti-Müllerian hormone expres-

sion, as related to DMRT1, SF-1, WT1, GATA-4, Wnt-4, and Lhx9 expression, in the chick differentiating gonads. Dev. Dyn. **225:** 221–232
16 Wegner M. (1999) From head to toes: the multiple facets of Sox proteins. Nucleic Acids Res. **15:** 1409–1420
17 Bowles J., Schepers G. and Koopman P. (2000) Phylogeny of the SOX family of developmental transcription factors based on sequence and structural indicators. Dev. Biol. 227: 239–255
18 Schepers G. E., Teasdale R. D. and Koopman P. (2002) Twenty pairs of Sox: extent, homology, and nomenclature of the mouse and human sox transcription factor gene families. Dev. Cell. **3:** 167–170
19 Foster J. W., Dominguez-Steglich M. A., Guioli S., Kowk C., Weller P. A., Weissenbach J. et al. (1994) Campomelic dysplasia and autosomal sex reversal caused by mutations in an SRY-related gene. Nature **372:** 525–30
20 Wagner T., Wirth J., Meyer J., Zabel B., Held M., Zimmer J. et al. (1994) Autosomal sex reversal and campomelic dysplasia are caused by mutations in and around the SRY-related gene SOX9. Cell **79:** 1111–120
21 Vidal V. P. I., Chaboissier M.-C., Rooij D. G. de and Schedl A. (2001) Sox9 induces testis development in XX transgenic mice. Nat. Genet. **28:** 216–17
22 Josso N., Clemente N. di and Gouédard L. (2001) Anti-Müllerian hormone and its receptors. Mol. Cell. Endocrinol. **179:** 25–32
23 Nachtigal M. W., Hirokawa Y., Enyeart-VanHouten D. L., Flanagan J. N., Hammer G. D. and Ingraham H. A. (1998) Wilms' tumor 1 and Dax-1 modulate the orphan nuclear receptor SF-1 in sex-specific gene expression. Cell **93:** 445–454
24 Tremblay J. J. and Viger R. S. (1999) Transcription factor GATA-4 enhances Müllerian inhibiting substance gene transcription through a direct interaction with the nuclear receptor SF-1. Mol. Endocrinol. **13:** 1388–1401
25 Santa Barbara P. de, Bonneaud N., Boizet B., Desclozeaux M., Moniot B., Südbeck P. et al. (1998) Direct interaction of SRY-related protein SOX9 and steroidogenic factor 1 regulates transcription of the human anti-Müllerian hormone gene. Mol. Cell. Biol. **18:** 6653–6665
26 Schepers G., Wilson M., Wilhelm D. and Koopman P. (2003) SOX8 is expressed during testis differentiation in mice and synergizes with SF1 to activate the Amh promoter in vitro. J. Biol. Chem. **278:** 28101–28108
27 Arango N. A., Lovell-Badge R. and Behringer R. R. (1999) Targeted mutagenesis of the endogenous mouse Mis gene promoter: in vivo definition of genetic pathways of vertebrate sexual development. Cell **99:** 409–419
28 Oréal E., Pieau C., Mattei M. G., Josso N., Picard J.-Y., Carré-Eusèbe D. et al. (1998) Early expression of AMH in chicken embryonic gonads precedes testicular SOX9 expression. Dev. Dyn. **212:** 522–532
29 Smith C. A., Smith M. J. and Sinclair A. H. (1999a) Gene expression during gonadogenesis in the chicken embryo. Gene **234:** 395–402
30 Takada S. and Koopman P. (2003) Origin and possible roles of the Sox8 transcription factor gene during sexual development. Cytogenet. Genome Res. **101:** 212–218
31 Schepers G. E., Bullejos M., Hosking B. M. and Koopman P. (2000) Cloning and characterisation of the Sry-related transcription factor gene Sox8. Nucleic Acids Res. **28:** 1473–1480
32 Wright E., Hargrave M. R., Christiansen J., Cooper L., Kun J., Evans T. et al. (1995) The Sry-related gene Sox-9 is expressed during chondrogenesis in mouse embryos. Nat. Genet. **9:** 15–20
33 Pusch C., Hustert E., Pfeifer D., Südbeck P., Kist R., Roe B. et al. (1998) The SOX10/Sox10 gene from human and mouse: sequence, expression, and transactivation by the encoded HMG domain transcription factor. Hum. Genet. **103:** 115–123
34 Collignon J., Sockanathan S., Hacker A., Cohen-Tannoudji M., Norris D., Rastan S. et al. (1996) A comparison of the properties of Sox-3 with Sry and two related genes, Sox-1 and Sox-2. Development **122:** 509–520
35 Smits P., Li P., Mandel J., Zhang Z., Deng J. M., Behringer R. R. et al. (2001) The transcription factors L-Sox5 and Sox6 are essential for cartilage formation. Dev Cell **1:** 277–290
36 Downes M. and Koopman P. (2001) SOX18 and the transcriptional regulation of blood vessel development. Trends Cardiovasc. Med. **11:** 318–324
37 Kanai-Azuma M., Kanai Y., Gad J. M., Tajima Y., Taya C., Kurohmaru M. et al. (2002) Depletion of definitive gut endoderm in Sox17-null mutant mice. Development **129:** 2367–2379
38 Pennisi D., Bowles J., Nagy A., Muscat G. and Koopman P. (2000) Mice null for Sox18 are viable and display a mild coat defect. Mol. Cell. Biol. **20:** 9331–9336
39 Hamburger V. and Hamilton H. L-. (1951) A series of normal stages in the development of the chick embryo. J. Morphol. **88:** 49–92
40 Clinton M., Haines L., Belloir B. and McBride D. (2001) Sexing chick embryos: a rapid and simple protocol. Br. Poult. Sci. **42:** 134–138
41 Chomczynski P. and Sacchi N. (1987) Single-step method of RNA isolation by acid guanidinium thiocyanate-phenol-chloroform extraction. Anal. Biochem. **162:** 156–159
42 Xu Q. and Wilkinson D. (1998) In situ hybridization of mRNA with hapten labelled probes. In: In Situ Hybridization: a Practical Approach, 2nd ed., pp. 87–106, Wilkinson D. (ed.), Oxford University Press, Oxford
43 Romanoff A. L. (1960) The Avian Embryo: Structural and Functional Development, Macmillan, New York
44 Bell K. M., Western P. S. and Sinclair A. H. (2000) SOX8 expression during chick embryogenesis. Mech. Dev. 94: 257–260
45 Maschhoff K. L., Anziano P. Q., Ward P. and Baldwin H. S. (2003) Conservation of Sox4 gene structure and expression during chicken embryogenesis. Gene **320:** 23–30
46 Uwanogho D., Rex M., Cartwright E. J., Pearl G., Healy C., Scotting P. J. et al. (1995) Embryonic expression of the chicken Sox2, Sox3 and Sox11 genes suggests an interactive role in neuronal development. Mech. Dev. **49:** 23–36
47 Healy C, Uwanogho D. and Sharpe P. T. (1999) Regulation and role of Sox9 in cartilage formation. Dev. Dyn. **215:** 69–78
48 Parker K. L. and Schimmer B. P. (1997) Steroidogenic factor 1: a key determinant of endocrine development and function. Endocr. Rev. **18:** 361–377
49 Takada S., DiNapoli L., Capel B. and Koopman P. (2004) Sox8 is expressed at similar levels in gonads of both sexes during the sex determining period in turtles. Dev. Dyn. **231:** 387–395
50 Pelletier J., Schalling M., Buckler A. J., Rogers A., Haber D. A. and Housman D. (1991) Expression of the Wilms' tumor gene WT1 in the murine urogenital system. Genes. Dev. **5:** 1345–1356
51 Birk O. S., Casiano D. E., Wassif C. A., Cogliati T., Zhao L., Zhao Y. et al. (2000) The LIM homeobox gene Lhx9 is essential for mouse gonad formation. Nature **403:** 909–913
52 Vainio S., Heikkila M., Kispert A., Chin N. and McMahon A. P. (1999) Female development in mammals is regulated by Wnt-4 signalling. Nature **397:** 405–409
53 Swain A., Zanaria E., Hacker A., Lovell-Badge R. and Camerino G. (1996) Mouse Dax1 expression is consistent with a role in sex determination as well as in adrenal and hypothalamus function. Nat. Genet. **12:** 404–409
54 Raymond C. S., Kettlewell J. R., Hirsch B., Bardwell V. J. and Zarkower D. (1999) Expression of Dmrt1 in the genital ridge of mouse and chicken embryos suggests a role in vertebrate sexual development. Dev. Biol. **215:** 208–220

ELSEVIER

International Journal of Cardiology 102 (2005) 233–238

International Journal of Cardiology

www.elsevier.com/locate/ijcard

Gene expression profiling of human atrial myocardium with atrial fibrillation by DNA microarray analysis

Ruri Ohki[a], Keiji Yamamoto[a,*], Shuichi Ueno[a], Hiroyuki Mano[b], Yoshio Misawa[c] Katsuo Fuse[c], Uichi Ikeda[a], Kazuyuki Shimada[a]

[a]*Division of Cardiovascular Medicine, Jichi Medical School, Minamikawachi-Machi, Tochigi 329-0498, Japan*
[b]*Division of Functional Genomics, Jichi Medical School, Minamikawachi-Machi, Tochigi 329-0498, Japan*
[c]*Division of Cardiovascular Surgery, Jichi Medical School, Minamikawachi-Machi, Tochigi 329-0498, Japan*

Received 16 December 2003; received in revised form 31 March 2004; accepted 5 May 2004
Available online 9 August 2004

Abstract

Background: Atrial fibrillation (AF) is the most frequently encountered arrhythmia in the clinical setting. However, a comprehensive investigation of the molecular mechanism of AF has not been performed. The aim of this study was to clarify transcriptional profiling of genes modulated in the atrium of AF patients using DNA microarray technology.
Methods: We obtained 17 fresh cardiac specimens, right atrial appendages, isolated from 10 patients with normal sinus rhythm and seven chronic AF patients who underwent cardiac surgery. Affymetrix GeneChip (Human Genome U95A) investigating 12,000 human genes was used for each specimen. Quantitative analysis of selected genes was performed by the real-time PCR method.
Results: The left atrial diameter in the AF group was greater than that in the sinus rhythm group. We could identify 33 AF-specific genes that were significantly activated (>1.5-fold), compared with the sinus rhythm group, including an ion channel, an antioxidant, an inflammation, three cell growth/cell cycle, three transcription such as nuclear factor-interleukin 6-beta, several cell signaling and several protein genes, and seven expressed sequence tags (ESTs). In contrast, we found 63 sinus rhythm-specific genes, including several cell signaling/communication such as sarcoplasmic reticulum Ca^{2+}-ATPase 2, several cellular respiration and energy production and two antiproliferative or negative regulator of cell growth genes, and 22 ESTs.
Conclusions: The present study demonstrated that about one hundred genes were modulated in the atria of AF patients. These findings suggest that these genes may play critical roles in the initiation or perpetuation of AF and the pathophysiology of atrial remodeling.

Keywords: Atrial fibrillation; Genes; Microarray; Myocardium

1. Introduction

Atrial fibrillation (AF) is the most common sustained cardiac arrhythmia and the major cardiac cause of stroke [1]. The Framingham Study [2] reported a sixfold increase in the incidence of stroke in patients with AF, compared with age-, sex-, and blood pressure-adjusted control subjects. In addition, the rapid heart rate resulting from AF can bring about a number of adverse outcomes including congestive heart failure and tachycardia-related cardiomyopathy [3,4]. The molecular research of AF has been focused mainly at various ion channels and at proteins involved in calcium homeostasis, because AF modifies the electrical properties of the atrium in a manner that promotes its occurrence and maintenance. This arrhythmogenic electrophysiological remodeling is well established. However, a comprehensive investigation of the molecular mechanism causing AF has not been performed.

With the recent discovery of the complete sequence of the human genome, as well as the genomes of other organisms, new high-throughput approaches to studying these complex pathways have been made possible. By

* Corresponding author. Tel.: +81 285 58 7344; fax: +81 285 44 5317.
E-mail address: kyamamoto@jichi.ac.jp (K. Yamamoto).

0167-5273/$ - see front matter © 2004 Elsevier Ireland Ltd. All rights reserved.
doi:10.1016/j.ijcard.2004.05.026

Table 1
Patient characteristics

Variable	Total (n=17)	AF (n=7)	Sinus rhythm (n=10)
Age (yrs)	59 ± 16	64 ± 9	56 ± 18
Left atrial diameter (mm)	52 ± 15	67 ± 9*	42 ± 7
LV ejection fraction (%)	60 ± 13	62 ± 13	58 ± 14
MR grade	2.2 ± 1.4	2.7 ± 1.0	1.8 ± 1.0
TR grade	2.0 ± 1.4	2.7 ± 1.0	1.5 ± 1.0
Systolic PA pressure (mmHg)	39.9 ± 14.0	45.0 ± 14.0	35.4 ± 14.0
Mean RA pressure (mmHg)	6.5 ± 3.5	8.6 ± 4.0	4.8 ± 1.0
Digitalis (n)	9	7	2
Systolic blood pressure (mmHg)	133 ± 25	134 ± 26	133 ± 25
Diastolic blood pressure (mmHg)	71 ± 16	75 ± 20	69 ± 13
Fasting blood sugar (mg/dl)	101 ± 15	90 ± 7†	107 ± 15
Total cholesterol (mg/dl)	195 ± 44	208 ± 41	189 ± 46
Triglyceride (mg/dl)	123 ± 64	118 ± 54	125 ± 71

Data are mean ±S.D. or n. *P<0.001 and †P<0.02 compared with sinus rhythm patients. AF, atrial fibrillation; LV, left ventricular; MR, mitral valve regurgitation; PA, pulmonary arterial; RA, right atrial; TR, tricuspid valve regurgitation.

using multiple cDNA or oligonucleotide samples placed on a glass slide, investigators can analyze several thousand full-length genes or expressed oligonucleotide sequences at once. In addition to identifying large clusters of genes that respond to a given stimulus, DNA microarray technology may be used to identify some genes that comprise highly specific molecular responses [5,6]. Already, some studies using microarray technology have yielded interesting results regarding the pathogenesis of cardiovascular diseases, such as myocardial infarction [7], cardiac hypertrophy [8], and human heart failure [9]. In the present study, we used DNA microarray technology to investigate the transcriptional profiling of genes modulated in the right atrium of patients with AF compared with sinus rhythm.

2. Methods

2.1. Subjects

This study group consisted of seven patients with AF (mean age 64±9 years) and 10 patients with sinus rhythm (mean age 56±18 years) who underwent cardiac surgery (Table 1). The underlying heart diseases in the patients are shown in Table 2. Hemodynamic studies were performed the morning after an overnight fast. Vasodilators were withheld for at least 24 h before evaluation. Chronic, stable doses of digoxin, and diuretics were continued but were administered on an evening schedule. Right and left heart studies, including measurement of pressure, biplane left ventriculography and coronary angiography, were performed using a percutaneous cathether. Left ventricular ejection fraction was determined by the area-length method [10]. The severity of mitral regurgitation was assessed according to the method of Sellers et al. [11]. Transthoracic echocardiography was performed in all patients using a Hewlett-Packard SONOS 5500 system (Hewlett-Packard, Palo Alto, CA) with a 2.5 MHz transducer. The left atrial diameter was determined by M-mode echocardiography [12]. The severity of tricuspid regurgitation was graded on a four-point scale, based on the distance reached by the abnormal signals from the tricuspid orifice toward the posterior wall in the parasternal four-chamber view [13].

This study was approved by our institutional human investigations committee, and written informed consent was obtained from all patients before participation.

2.2. Atrial myocardium samples

Right atrial appendages were obtained from the patients during cardiac surgery. Pieces of right atrial appendage weighing 200–1400 mg were frozen immediately in liquid nitrogen, and stored at −80 °C.

Table 2
Underlying heart disease

Patients	Age	Sex	Diagnosis
Sinus group			
1	44	M	AR
2	70	F	MR
3	75	M	AP
4	65	M	AS
5	60	M	AS
6	64	F	MR
7	64	F	AR, MR
8	15	M	ASD
9	63	M	AR
10	36	F	ASD
AF group			
1	51	F	MS
2	55	M	MR
3	64	M	MR
4	74	F	ASR, MSR
5	75	M	ASR, MR
6	59	F	MS
7	69	F	MSR

AP, angina pectoris; AR, aortic valve regurgitation; AS, aortic valve stenosis; ASD, atrial septal defect; ASR, aortic valve stenosis and regurgitation; MR, mitral valve regurgitation; MS, mitral valve stenosis; MSR, mitral valve stenosis and regurgitation.

2.3. Transcriptional profiling

A DNA microarray was used for each specimen. Total RNA was extracted using RNAzol B (TEL-TEST, Friendswood, TX), and the purity was checked by spectrophotometry and agarose gel electrophoresis. Total RNA (5 μg) was converted to double-stranded cDNA using an oligo dT primer containing the T7 promoter (Gibco BRL Superscript® Choice System; Life Technologies, Rockville, MD), and the template for an in vitro transcription reaction was used to synthesize biotin-labeled antisense cRNA (Bio-Array™ High Yield RNA Transcript Labeling Kit; Enzo Diagnostics, Farmingdale, NY). The biotinylated cRNA was fragmented and hybridized for 16 h at 45 °C to GeneChip Test2 arrays (Affymetrix, Santa Clara, CA) to assess sample quality, and then to Human Genome arrays (U95A, Affymetrix). The arrays were washed, and then stained with streptavidin-phycoerythrin. The arrays were scanned with the GeneArray scanner (Agilent Technologies, Palo Alto, CA) and analyzed using the GeneSpring software package (Silicon Genetics, Redwood City, CA). Human Genome U95A was derived from GenBank 113 and dbEST/10-02-99.

Detailed protocols for data analysis of Affymetrix oligonucleotide microarrays and extensive documentation of the sensitivity and quantitative aspects of the method have been described [14–16]. Briefly, each gene is represented by the use of ~20 perfectly matched (PM) and mismatched (MM) control probes. The MM probes act as specificity controls that allow the direct subtraction of both background and cross-hybridization signals. The number of instances in which the PM hybridization signal is larger than the MM signal is computed along with the average of the logarithm of the PM:MM ratio (after background subtraction) for each probe set. These values are used to make a matrix-based decision concerning the presence or absence of an RNA molecule. Positive average signal intensities after background subtraction were observed for over 12,000 genes for all samples. To determine the quantitative RNA abundance, the average of the differences representing PM minus MM for each gene-specific probe family is calculated, after discarding the maximum, the minimum, and any outliers beyond 3 SDs.

2.4. Real-time reverse transcription (RT)-PCR analysis

For reverse transcription (RT), RNA obtained from each specimen was reverse transcribed using T7-dT primer (5′-TCT AGT CGA CGG CCA GTG AAT TGT AAT ACG ACT CAC TAT AGG GCG TTT TTT TTT TTT TTT TTT TTT-3′) and Superscript II reverse transcriptase (Life Technologies). Real-time quantitative PCR was performed in optical tubes in a 96-well microtiter plate (Perkin-Elmer/Applied Biosystems, Foster City, CA) with an ABI PRISM 7700 Sequence Detector Systems (Perkin-Elmer/Applied Biosystems) according to the manufacturer's instructions. By using the SYBR Green PCR Core Reagents Kit (Perkin-Elmer/Applied Biosystems, P/N 4304886), fluorescence signals were generated during each PCR cycle via the 5′-to 3′-endonuclease activity of Taq Gold [17] to provide real-time quantitative PCR information. The oligonucleotide primers used for real-time PCR analysis are shown in Table 3. No template controls as well as the samples were added in a total volume of 50 μl/reaction. Potential PCR product contamination was digested by uracil-*N*-glycosylase, because dTTP is substituted by dUTP [17]. All PCR experiments were performed with the hot start method. In the reaction system, uracil-*N*-glycosylase and Taq Gold (Perkin-Elmer/Applied Biosystems) were applied according to the manufacturer's instructions [17,18]. Denaturing and annealing reactions were performed 40 times at 95 °C for 15 s, and at 60 °C for sarcoplasmic reticulum Ca^{2+}-ATPase 2, 66 °C for nuclear factor-interleukin 6 (NF-IL6)-beta and 62 °C for glyceraldehyde-3 phosphate dehydrogenase (GAPDH) for 1 min, respectively. The increase in the fluorescence signal is proportional to the amount of specific product [14]. The intensity of emission signals in each sample was normalized to that of GAPDH as an internal control.

2.5. Statistical analysis

Raw data from array scans were averaged across all gene probes for each array, and a scaling factor was applied to bring the average intensity for all probes on the array to 2500. This allows any sample to be normalized for comparison with any other comparable sample.

Table 3
Primer design for real-time PCR analysis

Gene		Primer sequence	PCR product size (bp)
NF-IL6-beta	Sense	5′-CACAGACCGTGGTGAGCTTG-3′	257
	Antisense	5′-CACCAACTTCTGCTGCATCTC-3′	
Sarcoplasmic reticulum	Sense	5′-TTTCTGGTACAAACATTGCTGC-3′	140
Ca^{2+}-ATPase 2	Antisense	5′-TAGTTTTTGCTGAAGGGGTGTT-3′	
GAPDH	Sense	5′-CTTTGGTATCGTGGAAGGACTC-3′	140
	Antisense	5′-CAGTAGAGGCAGGGATGATGTT-3′	

GAPDH, glyceraldehyde-3 phosphate dehydrogenase; NF-IL6, nuclear factor-interleukin 6.

Table 4
Analysis of AF-specific genes by DNA microarray

Function	Gene	Fold change	Genbank#
Antioxidants	Glutathione peroxidase	1.8 ± 1.1	X13710
Cell growth	Vascular endothelial growth factor B	1.6 ± 0.7	U43368
Cell signaling	RhoC	1.6 ± 0.5	L25081
Inflammation	Macrophage migration inhibitory factor	1.7 ± 0.6	L19686
Proto-oncogene	A-raf-1 oncogene	1.5 ± 0.5	U01337
Transcription	NF-IL6-beta	2.0 ± 0.7	M83667

Data are mean ±S.D. Fold change was relative to sinus rhythm group. NF-IL6, nuclear factor-interleukin 6.

Data are expressed as the mean ± S.D. Differences were analyzed with the Mann–Whitney *U* test for unpaired observations. A *P*-value of <0.05 was considered significant.

3. Results

3.1. Patient characteristics

As shown in Table 1, the left atrial diameter in the AF group was significantly greater than that in the sinus rhythm group ($P<0.001$). In addition, the levels of fasting blood sugar in the AF group were significantly lower than those in the sinus rhythm group ($P<0.02$). There were no other differences detected between the sinus rhythm group and AF group.

3.2. DNA microarray analysis of AF-specific genes

We identified 33 AF-specific genes that were significantly activated (>1.5-fold, $P<0.05$), compared with those in the sinus rhythm group, including an ion channel, an antioxidant, an inflammation, three cell growth/cell cycle, three transcription, several cell signaling and several protein genes, and seven expressed sequence tags (ESTs). Some of the selected genes are shown in Table 4. All data are available in an online only Data Supplement at http://www.elsevier.com/locate/inca/506041.

3.3. DNA microarray analysis of sinus rhythm-specific genes

In contrast, we found 63 sinus rhythm-specific genes, including several cell signaling/communication genes such as sarcoplasmic reticulum Ca^{2+}-ATPase 2, several cellular respiration and energy production and two antiproliferative or negative regulator of cell growth genes, and 22 ESTs (<0.5-fold, $P<0.05$). Some of the selected genes are shown in Table 5. All data are available in an online only Data Supplement at http://www.elsevier.com/locate/inca/506041.

3.4. Real-time RT-PCR analysis

We focused on two of the genes screened by the oligonucleotide microarray: NF-IL6-beta and sarcoplasmic reticulum Ca^{2+}-ATPase 2. NF-IL6-beta is an important transcriptional activator in the regulation of genes involved in the immune and inflammatory response [19]. AF may persist due to structural changes in the atria that are promoted by inflammation [20]. In addition, cytosolic Ca^{2+} overload may be an important mediator of AF. Abnormalities in the Ca^{2+} regulatory proteins, such as sarcoplasmic reticulum Ca^{2+}-ATPase 2, of the atrial myocardium in chronic AF patients may be involved in the initiation and/or perpetuation of AF. These genes were confirmed by the real-time RT-PCR method. As shown in Fig. 1, NF-IL6-beta mRNA expression in the AF group was significantly higher than that in the sinus rhythm group ($P<0.02$). In contrast, as shown in Fig. 2, sarcoplasmic reticulum Ca^{2+}-ATPase 2 mRNA expression in the AF group was lower compared with that in the sinus rhythm group ($P<0.1$), but not significantly.

4. Discussion

The cellular and molecular basis of AF has been a field of enormous interest over the past few years. However, the

Table 5
Analysis of sinus rhythm-specific genes by DNA microarray

Function	Gene	Fold change	Genbank#
Antioxidants	Peroxiredoxin 3	0.5 ± 0.2	D49396
Cell signaling	Caveolin 2	0.4 ± 0.3	AF035752
Cell signaling	Sarcoplasmic reticulum Ca^{2+}-ATPase 2	0.4 ± 0.3	M23115
Cell signaling	Connexin 43	0.4 ± 0.3	X52947
Proto-oncogene	Ras-associated protein rab1	0.5 ± 0.2	AL050268

Data are mean ±S.D. Fold change was relative to sinus rhythm group.

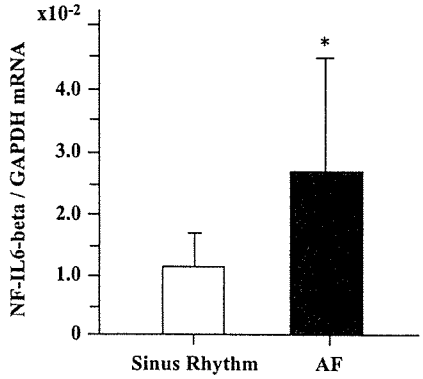

Fig. 1. Nuclear factor-interleukin 6 (NF-IL6)-beta mRNA expression in the right atria of patients with sinus rhythm and atrial fibrillation (AF). Total RNA obtained from the right atria of patients with sinus rhythm (n=10) and AF (n=7) using RNAzol B (TEL-TEST) was analyzed by quantitative real-time reverse transcription-PCR as described in Methods. The amount of mRNA expression for NF-IL6-beta was standardized to that of glyceraldehyde-3 phosphate dehydrogenase (GAPDH) mRNA expression. Data are means±S.D. *P<0.02 compared with sinus rhythm patients.

mechanism of AF in human tissues is extremely complex, because atrial remodeling consists of electrical, contractile, and structural remodeling. In addition, structural remodeling may occur from chronic hemodynamic, metabolic, or inflammatory stressors. Many factors such as ion channels, proteins influencing calcium homeostasis, connexins, autonomic innervation, fibrosis, paracrine factors, and cytokines may be involved in the molecular mechanism of AF. The present study using oligonucleotide microarray analysis demonstrated that about one hundred genes were modulated in the right atrium of patients with AF. These findings suggest that these genes may play critical roles in the initiation or perpetuation of AF and the pathophysiology of atrial remodeling.

In the present study, DNA microarray analysis identified 33 AF-specific genes. Some of these genes encode NF-IL6-beta, macrophage migration inhibitory factor, A-raf-1 oncogene, vascular endothelial growth factor B, RhoC, and glutathione peroxidase. NF-IL6-beta mRNA expression induced in the atria of AF patients was confirmed by the real-time PCR method. NF-IL6-beta and macrophage migration inhibitory factor are involved in inflammation [19,21]. Chung et al. [20] reported that C-reactive protein, a marker of systemic inflammation, is elevated in AF patients compared with sinus rhythm patients. Novel and inflammatory mechanisms may promote the persistence of AF, potentially by inducing structural and/or electrical remodeling of the atria. A-raf-1 protooncogene encodes cytoplasmic protein serine/threonine kinase, which plays an important role in cell growth and development [22]. Vascular endothelial growth factor B with structural similarities to vascular endothelial growth factor and placenta growth factor has a role in angiogenesis and endothelial cell growth [23]. RhoC, small guanosine triphosphatase Rho, which regulates remodeling of the actin cytoskeleton during cell morphogenesis and motility [24], may contribute to the structural remodeling. Baumer et al. [25] demonstrated that the activity, mRNA, and protein levels of glutathione peroxidase, an antioxidative enzyme, decreased in human failing myocardium. However, the present study showed that the glutathione peroxidase mRNA level in AF patients was elevated.

The present study demonstrated that the expression of 63 genes in AF patients was significantly lower compared with sinus rhythm. For example, genes for sarcoplasmic reticulum Ca^{2+}ATPase 2 and connexin 43 in AF patients were downregulated. In the real-time PCR analysis, sarcoplasmic reticulum Ca^{2+}-ATPase 2 mRNA expression in the AF group was lower compared with that in the sinus rhythm group, but not significantly. Ohkusa et al. [26] also reported that sarcoplasmic reticulum Ca^{2+}-ATPase 2 mRNA in both the right and left atrial myocardial tissues from 13 patients with AF were significantly lower than in the right atrium of patients with sinus rhythm. A decrease in sarcoplasmic reticulum Ca^{2+}-ATPase 2 in the atria may sustain abnormal intracellular Ca^{2+} handling and changes in the electrophysiologic properties of atrial tissue, leading to the perpetuation of AF. Connexin 43 is one of the gap junctions that are clusters of closely packed channels. Gap junctions directly connect the cytoplasmic compartments of neighboring cells and allow the passage of ions and small molecules. In the present study, connexin 43 mRNA expression in AF patients was downregulated. It is still controversial whether connexin 43 is upregulated [27], unchanged or downregulated in AF. Thus, changes in the expressions of connexin 43 might affect conduction velocity, contributing to sustained AF.

Previous studies demonstrated that some genes including L-type calcium channel [28], potassium channels [29], and sarcoplasmic reticulum Ca^{2+}-ATPase 2 [26,28] are modulated in AF patients. However, the molecular

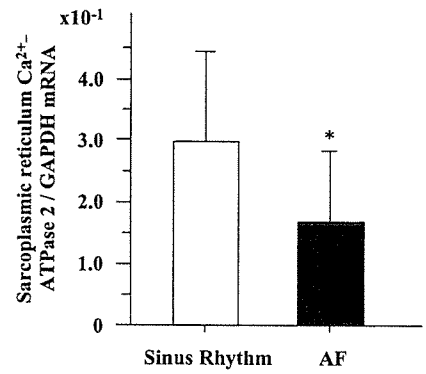

Fig. 2. Sarcoplasmic reticulum Ca^{2+}-ATPase 2 mRNA expression in the right atria of patients with sinus rhythm and atrial fibrillation (AF). Total RNA obtained from the right atria of patients with sinus rhythm (n=10) and AF (n=7) using RNAzol B (TEL-TEST) was analyzed by quantitative real-time reverse transcription-PCR as described in Methods. The amount of mRNA expression for sarcoplasmic reticulum Ca^{2+}-ATPase 2 was standardized to that of glyceraldehyde-3 phosphate dehydrogenase (GAPDH) mRNA expression. Data are means±S.D. *P<0.1 compared with sinus rhythm patients.

mechanism of AF is poorly understood. Although the roles of other genes including ESTs in the heart except for the genes described above still remain unknown, the genes screened in this study may provide insights into the initiation or perpetuation of AF and the pathophysiology of atrial remodeling, because DNA microarray is a highly effective method for screening genes.

Acknowledgements

This study was supported by grants from the Ministry of Education, Science, Sports and Culture of Japan (15590769), Tokyo, Japan, the Mitsui Life Social Welfare Foundation, Tokyo, Japan, the Takeda Science Foundation, Osaka, Japan, the Daiwa Securities Health Foundation, Tokyo, Japan, and the Sankyo Foundation of Life Science, Tokyo, Japan.

References

[1] Cerebral Embolism Task Force. Cardiogenic brain embolism. Arch Neurol 1986;43:71–84.
[2] Wolf PA, Dawber TR, Thomas Jr HE, Kannel WB. Epidemiologic assessment of chronic atrial fibrillation and risk of stroke: the Framingham study. Neurology 1978;28:973–7.
[3] Okishige K, Sasano T, Yano K, Azegami K, Suzuki K, Itoh K. Serious arrhythmias in patients with apical hypertrophic cardiomyopathy. Intern Med 2001;40:396–402.
[4] Redfield MM, Kay GN, Jenkins LS, Miánulli M, Jensen DN, Ellenbogen KA. Tachycardia-related cardiomyopathy: a common cause of ventricular dysfunction in patients with atrial fibrillation referred for atrioventricular ablation. Mayo Clin Proc 2000;75:790–5.
[5] Iyer VR, Eisen MB, Ross DT, et al. The transcriptional program in the response of human fibroblasts to serum. Science 1999;283:83–7.
[6] Feng Y, Yang JH, Huang H, et al. Transcriptional profile of mechanically induced genes in human vascular smooth muscle cells. Circ Res 1999;85:1118–23.
[7] Stanton LW, Garrard LJ, Damm D, et al. Altered patterns of gene expression in response to myocardial infarction. Circ Res 2000;86:939–45.
[8] Friddle CJ, Koga T, Rubin EM, Bristow J. Expression profiling reveals distinct sets of genes altered during induction and regression of cardiac hypertrophy. Proc Natl Acad Sci U S A 2000;97:6745–50.
[9] Yang J, Moravec CS, Sussman MA, et al. Decreased SLIM1 expression and increased gelsolin expression in failing human hearts measured by high-density oligonucleotide arrays. Circulation 2000;102:3046–52.
[10] Greene DG, Carlisle R, Grant C, Bunnell IL. Estimation of left ventricular volume by one-plane cineangiography. Circulation 1967;35:61–9.
[11] Sellers RD, Levy MJ, Amplatz K, Lillehei CW. Left retrograde cardioangiography in acquired cardiac disease: technic, indications and interpretation in 700 cases. Am J Cardiol 1964;14:437–47.
[12] Sahn DJ, DeMaria A, Kisslo J, Weyman A. Recommendations regarding quantitation in M-mode echocardiography: results of a survey of echocardiographic measurements. Circulation 1978;58: 1072–1083.
[13] Miyatake K, Okamoto M, Kinoshita N, et al. Evaluation of tricuspid regurgitation by pulsed Doppler and two-dimensional echocardiography. Circulation 1982;66:777–89.
[14] Lockhart DJ, Dong H, Byrne MC, et al. Expression monitoring by hybridization to high-density oligonucleotide arrays. Nat Biotechnol 1996;14:1675–80.
[15] Lee CK, Klopp RG, Weindruch R, Prolla TA. Gene expression profile of aging and its retardation by caloric restriction. Science 1999; 285:1390–3.
[16] Golub TR, Slonim DK, Tamayo P, et al. Molecular classification of cancer: class discovery and class prediction by gene expression monitoring. Science 1999;286:531–7.
[17] Heid CA, Stevens J, Livak KJ, Williams PM. Real time quantitative PCR. Genome Res 1996;6:986–94.
[18] Kruse N, Pette M, Toyka K, Rieckmann P. Quantification of cytokine mRNA expression by RT PCR in samples of previously frozen blood. J Immunol Methods 1997;210:195–203.
[19] Kinoshita S, Akira S, Kishimoto T. A member of the C/EBP family, NF-IL6 beta, forms a heterodimer and transcriptionally synergizes with NF-IL6. Proc Natl Acad Sci U S A 1992;89:1473–6.
[20] Chung MK, Martin DO, Sprecher D, et al. C-reactive protein elevation in patients with atrial arrhythmias: inflammatory mechanisms and persistence of atrial fibrillation. Circulation 2001;104:2886–91.
[21] Bacher M, Metz CN, Calandra T, et al. An essential regulatory role for macrophage migration inhibitory factor in T-cell activation. Proc Natl Acad Sci U S A 1996;93:7849–54.
[22] Lee JE, Beck TW, Brennscheidt U, DeGennaro LJ, Rapp UR. The complete sequence and promoter activity of the human A-raf-1 gene (ARAF1). Genomics 1994;20:43–55.
[23] Olofsson B, Pajusola K, Kaipainen A, et al. Vascular endothelial growth factor B, a novel growth factor for endothelial cells. Proc Natl Acad Sci U S A 1996;93:2576–81.
[24] Maekawa M, Ishizaki T, Boku S, et al. Signaling from Rho to the actin cytoskeleton through protein kinases ROCK and LIM-kinase. Science 1999;285:895–8.
[25] Baumer AT, Flesch M, Wang X, Shen Q, Feuerstein GZ, Bohm M. Antioxidative enzymes in human hearts with idiopathic dilated cardiomyopathy. J Mol Cell Cardiol 2000;32:121–30.
[26] Ohkusa T, Ueyama T, Yamada J, et al. Alterations in cardiac sarcoplasmic reticulum Ca^{2+} regulatory proteins in the atrial tissue of patients with chronic atrial fibrillation. J Am Coll Cardiol 1999;34:255–63.
[27] van der Velden HM, Ausma J, Rook MB, et al. Gap junctional remodeling in relation to stabilization of atrial fibrillation in the goat. Cardiovasc Res 2000;46:476–86.
[28] Brundel BJ, van Gelder IC, Henning RH, et al. Gene expression of proteins influencing the calcium homeostasis in patients with persistent and paroxysmal atrial fibrillation. Cardiovasc Res 1999;42:443–54.
[29] Brundel BJ, VanGelder IC, Henning RH, et al. Alterations in potassium channel gene expression in atria of patients with persistent and paroxysmal atrial fibrillation: differential regulation of protein and mRNA levels for K+channels. J Am Coll Cardiol 2001;37:926–32.

Oncogene (2006) 25, 139–146

www.nature.com/onc

SHORT COMMUNICATION

Epigenetic silencing of *AXIN2* in colorectal carcinoma with microsatellite instability

K Koinuma[1,2], Y Yamashita[1], W Liu[3], H Hatanaka[1], K Kurashina[1,2], T Wada[1], S Takada[1], R Kaneda[1], YL Choi[1], S-I Fujiwara[1], Y Miyakura[2], H Nagai[2] and H Mano[1,4]

[1]Division of Functional Genomics, Jichi Medical School, Tochigi, Japan; [2]Department of Surgery, Jichi Medical School, Tochigi, Japan; [3]Division of Experimental Pathology, Mayo Clinic and Mayo Medical School, Rochester, MN, USA and [4]CREST, Japan Science and Technology Agency, Saitama, Japan

Mutation or epigenetic silencing of mismatch repair genes, such as *MLH1* and *MSH2*, results in microsatellite instability (MSI) in the genome of a subset of colorectal carcinomas (CRCs). However, little is yet known of genes that directly contribute to tumor formation in such cancers. To characterize MSI-dependent changes in gene expression, we have now compared transcriptomes between fresh CRC specimens positive or negative for MSI ($n = 10$ for each) with the use of high-density oligonucleotide microarrays harboring >44 000 probe sets. Correspondence analysis of the expression patterns of isolated MSI-associated genes revealed that the transcriptome of MSI$^+$ CRCs is clearly distinct from that of MSI$^-$ CRCs. Such MSI-associated genes included that for AXIN2, an important component of the WNT signaling pathway. *AXIN2* was silenced, apparently as a result of extensive methylation of its promoter region, specifically in MSI$^+$ CRC specimens. Forced expression of *AXIN2*, either by treatment with 5′-azacytidine or by transfection with *AXIN2* cDNA, resulted in rapid cell death in an MSI$^+$ CRC cell line. These data indicate that epigenetic silencing of *AXIN2* is specifically associated with carcinogenesis in MSI$^+$ CRCs.

Oncogene (2006) **25**, 139–146. doi:10.1038/sj.onc.1209009; published online 10 October 2005

Keywords: epigenetics; colorectal carcinoma; microsatellite instability; AXIN2; MLH1

Colorectal carcinoma (CRC) is one of the leading causes of cancer death in humans. Evidence indicates the existence of two major types of genomic instability in CRCs: chromosomal instability and microsatellite instability (MSI) (Lengauer *et al.*, 1998). Whereas chromosomal instability is associated with an abnormal DNA content (such as aneuploidy), inactivation of the tumor suppressor gene *TP53*, and activation of oncogenes (Kinzler and Vogelstein, 1996), MSI is associated with defects in DNA mismatch repair (MMR) that result in frameshift mutations in microsatellite repeats and thereby affect the structure of genes containing such repeats (Ionov *et al.*, 1993).

Although germline mutations of MMR genes have been detected in the genome of individuals with hereditary nonpolyposis colorectal cancer (Fishel *et al.*, 1993; Bronner *et al.*, 1994; Papadopoulos *et al.*, 1994), many sporadic CRCs positive for MSI are associated with epigenetic silencing of nonmutated MMR genes (Toyota *et al.*, 1999; Miyakura *et al.*, 2001). MSI$^+$ CRCs are characterized by specific clinicopathologic features and gene mutations. They occur with a higher frequency in women than in men, develop in the right side of the colon, and manifest a mucinous or poorly differentiated histopathology. Many of the CpG dinucleotides within the promoter region of the MMR gene *MLH1* are methylated (Cunningham *et al.*, 1998; Veigl *et al.*, 1998) and the *BRAF* gene frequently contains activating mutations (Koinuma *et al.*, 2004) in MSI$^+$ CRCs. Multiple genomic fragments have been found to be methylated in such CRCs (Toyota *et al.*, 1999), and an entity of CRC with a CpG island methylator phenotype has been proposed (Issa, 2004). The repertoire of genes that become methylated specifically in CRCs positive for *MLH1* methylation has remained uncharacterized, however.

To characterize directly the transcriptome specifically associated with MSI$^-$ CRC, we have now compared transcriptomes between fresh CRC specimens with or without MSI. Unexpectedly, we found that the expression of *AXIN2*, which encodes a component of the WNT signaling pathway, was markedly suppressed among the former tumors. CpG sequences within the *AXIN2* promoter were revealed to be extensively methylated in such CRCs. Forced expression of *AXIN2* inhibited cell proliferation in an MSI$^+$ CRC cell line, indicating that loss of *AXIN2* transcription is directly associated with carcinogenesis in MSI$^+$ CRCs.

To identify genes whose expression is specifically altered in MSI$^+$ CRCs, we first compared the transcriptomes of CRCs with or without MSI. A total of 248 consecutive cases of CRC were examined for MSI status

Correspondence: Professor H Mano, Division of Functional Genomics, Jichi Medical School, 3311-1 Yakushiji, Kawachigun, Tochigi 329-0498, Japan.
E-mail: hmano@jichi.ac.jp
Received 28 April 2005; revised 7 July 2005; accepted 13 July 2005; published online 10 October 2005

as well as for methylation of the promoter region of *MLH1* (Koinuma *et al.*, 2004). Most ($n=213$) of the cancer specimens were MSI$^-$, with the remainder ($n=35$) being positive for MSI. To compare the transcriptomes of these two subtypes of CRC, we randomly selected 10 specimens from each group and subjected them to gene expression profiling with microarrays (Affymetrix GeneChip HGU133) that harbor >44 000 probe sets. The clinical characteristics of the patients whose CRC specimens were subjected to microarray analysis are summarized in Table 1.

To exclude transcriptionally silent genes from our analyses, we first chose probe sets that received the 'Present' call from Microarray Suite 5.0 (Affymetrix) in at least 10% ($n=2$) of the samples. Two-way hierarchical clustering (Alon *et al.*, 1999) of the 20 patients based on the expression profiles of the isolated 21 888 probe sets failed to separate those with MSI$^+$ CRC from those with MSI$^-$ CRC (data not shown). We therefore attempted to identify 'MSI-associated probe sets' whose expression intensities differed significantly (Student's *t*-test, $P<0.001$) between the two classes and whose effect size (absolute difference in mean expression level) was $\geqslant 50$ U. Two-way clustering analysis with the 24 probe sets that fulfilled both these criteria clearly separated the individuals of the two clinical classes (Figure 1a). The distinct transcriptomes of the two classes were also confirmed by correspondence analysis (Fellenberg *et al.*, 2001), which reduced the complexity of the gene expression patterns from 24 to three dimensions. Projection of the study subjects into a virtual three-dimensional space based on their calculated coordinates revealed that the MSI$^+$ specimens were positioned apart from the MSI$^-$ ones (Figure 1b). These data indicate that the two classes of CRC possess distinct gene expression profiles, or 'molecular signatures', and they also suggest the feasibility of gene expression-based differential diagnosis of the two CRC subtypes.

Table 1 Clinical characteristics of the study subjects enrolled in microarray analysis

Patient ID	*Age (years)*	*Sex*	*MSI status*	MLH1 *methylation*	BRAF *gene*	KRAS2 *gene*	*Tumor site*	*Dukes stage*	*Pathology*	AXIN2 *methylation*
225	83	Female	Positive	Yes	Mutant	Wild	Proximal	C	Well	Yes
263	86	Female	Positive	Yes	Mutant	Wild	Proximal	C	Mod	Yes
280	83	Female	Positive	Yes	Mutant	Wild	Proximal	C	Well	Yes
305	74	Male	Positive	Yes	Mutant	Wild	Proximal	B	Sig	No
318	76	Female	Positive	Yes	Mutant	Wild	Proximal	B	Well	Yes
336	68	Male	Positive	Yes	Mutant	Wild	Proximal	B	Muc	No
413	69	Female	Positive	Yes	Mutant	Wild	Proximal	A	Well	No
416	76	Female	Positive	Yes	Mutant	Wild	Proximal	B	Muc	No
433	54	Female	Positive	Yes	Wild	Wild	Proximal	D	Well	Yes
479	74	Female	Positive	Yes	Mutant	Wild	Proximal	B	Mod	No
238	74	Male	Negative	No	Wild	Mutant	Distal	A	Well	No
249	62	Male	Negative	No	Wild	Wild	Proximal	B	Well	No
278	73	Male	Negative	No	Wild	Wild	Proximal	C	Well	No
295	71	Female	Negative	No	Wild	Mutant	Proximal	C	Well	No
298	70	Male	Negative	No	Wild	Mutant	Proximal	D	Well	No
307	80	Female	Negative	No	Wild	Wild	Proximal	C	Mod	No
308	62	Male	Negative	No	Wild	Wild	Distal	B	Mod	No
319	53	Female	Negative	No	Wild	Wild	Distal	A	Well	No
419	45	Female	Negative	No	Wild	Mutant	Proximal	D	Muc	No
426	42	Female	Negative	No	Wild	Wild	Proximal	C	Well	No

Well = well-differentiated adenocarcinoma; Mod = moderately differentiated adenocarcinoma; Sig = signet ring cell adenocarcinoma; Muc = mucinous adenocarcinoma. Methylation of *AXIN2* promoter region was determined by COBRA method.

Figure 1 Comparison of transcriptomes between CRCs positive or negative for MSI. (**a**) Subject tree generated by two-way clustering analysis with 24 probe sets that contrasted the two clinical conditions ($P<0.001$; effect size, $\geqslant 50$ U). Tumor samples were obtained from individuals with sporadic CRC who underwent surgical treatment at Jichi Medical School Hospital. Written informed consent was obtained from all patients, and the present study was approved by the ethics committee of Jichi Medical School. Microsatellite stability was determined by analysis of nine microsatellite repeat loci (three dinucleotide repeats and six mononucleotide repeats) as described previously (Miyakura *et al.*, 2001), and MSI status was stratified according to the criteria of the National Cancer Institute workshop (Boland *et al.*, 1998). Total RNA was extracted from ~100 mg of tissue, and was used in the hybridization experiments with GeneChip HGU133 A&B microarrays (Affymetrix), which harbor >44 000 probe sets corresponding to ~33 000 human genes, as described previously (Ohki-Kaneda *et al.*, 2004). The mean expression intensity of the internal positive control probe sets (http://www.affymetrix.com/support/technical/mask_files.affx) on the microarrays was set to 500 units (U) in each hybridization, and the fluorescence intensity of each probe set was normalized accordingly. All normalized array data are available at the Gene Expression Omnibus website (http://www.ncbi.nlm.nih.gov/geo) under the Accession Number GSE2138. Each column corresponds to a separate sample (MSI$^-$, green; MSI$^+$, red), and each row to a probe set whose expression is color-coded according to the indicated scale. Gene symbols are shown on the right; 225541_at, 226545_at, and 242414_at are expressed sequence tag IDs designated by Affymetrix (http://www.affymetrix.com). Annotations and expression intensities for the probe sets are presented in Supplementary Table 1. Note that *MLH1* expression was specifically suppressed in the MSI$^+$ samples. (**b**) Samples were projected into a virtual space with coordinates calculated by correspondence analysis of the 24 probe sets shown in (**a**). Correspondence analysis was performed with ViSta software (http://www.visualstats.org) for all genes showing a significant difference.

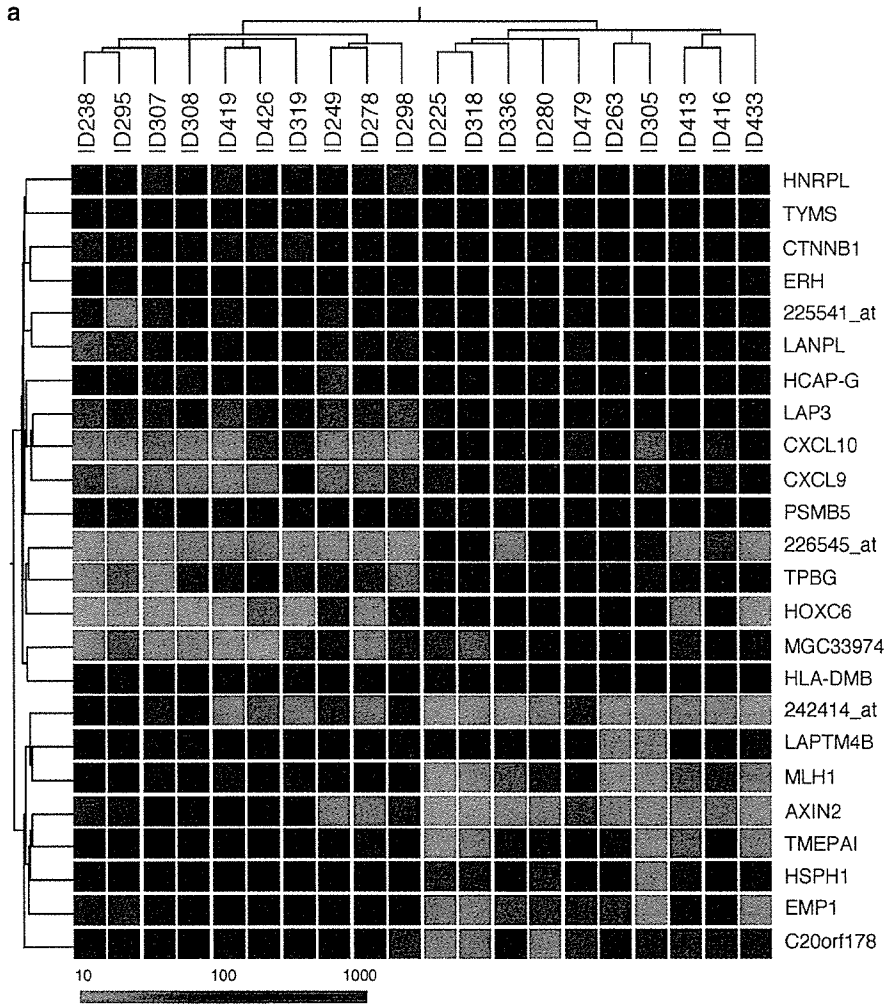
a
ID238
ID295
ID307
ID308
ID419
ID426
ID319
ID249
ID278
ID298
ID225
ID318
ID336
ID280
ID479
ID263
ID305
ID413
ID416
ID433
HNRPL
TYMS
CTNNB1
ERH
225541_at
LANPL
HCAP-G
LAP3
CXCL10
CXCL9
PSMB5
226545_at
TPBG
HOXC6
MGC33974
HLA-DMB
242414_at
LAPTM4B
MLH1
AXIN2
TMEPAI
HSPH1
EMP1
C20orf178
10
100
1000

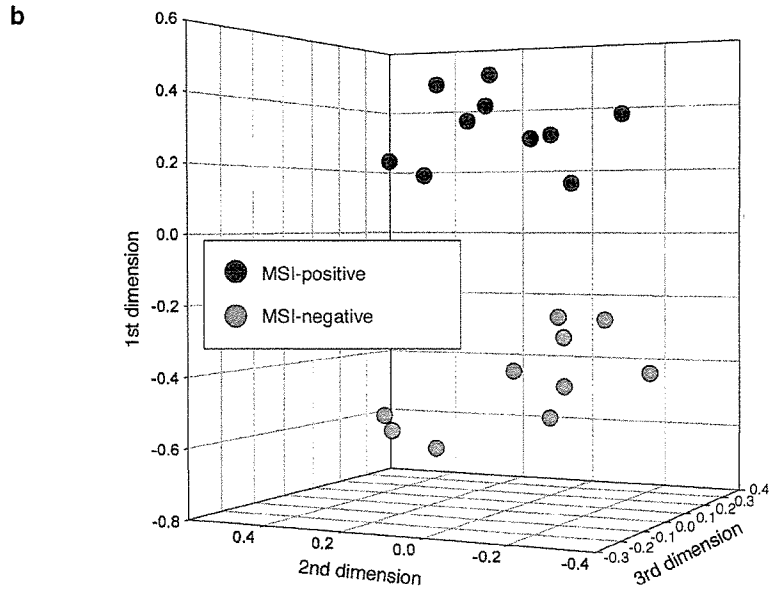
b
0.6
0.4
0.2
0.0
-0.2
-0.4
-0.6
-0.8
1st dimension
MSI-positive
MSI-negative
0.4
0.2
0.0
-0.2
-0.4
2nd dimension
-0.3
-0.2
-0.1
0.0
0.1
0.2
0.3
0.4
3rd dimension

The isolated MSI-associated genes include *AXIN2* and *CTNNB1* (β-catenin), both of which encode key participants in the WNT signaling pathway (Tolwinski and Wieschaus, 2004). Dysregulation of ubiquitin-dependent degradation of β-catenin contributes to carcinogenesis in a variety of CRCs and hepatocellular carcinomas (Narayan and Roy, 2003). AXIN2, similar to AXIN1, functions as a scaffold protein to facilitate this ubiquitination process by recruiting adenomatous polyposis coli (APC), glycogen synthase kinase-3β, and β-catenin (Behrens *et al*., 1998). Defects in the degradation of β-catenin have been shown to result from mutations in *AXIN1*, *AXIN2*, *APC*, or *CTNNB1* (Rubinfeld *et al*., 1997; Liu *et al*., 2000; Satoh *et al*., 2000; Smith *et al*., 2002). Our data therefore suggest that transcriptional suppression of *AXIN2* might represent a novel mechanism by which the function of the APC-AXIN–β-catenin complex is impaired in CRC.

To confirm the MSI-associated change in *AXIN2* expression, we measured the abundance of the corresponding mRNA in the original 20 study specimens by quantitative reverse transcription–polymerase chain reaction (RT–PCR) analysis (Figure 2a). Comparison of the amount of *AXIN2* mRNA determined by RT–PCR with that determined by microarray analysis yielded a Pearson's correlation coefficient (r) of 0.89, indicating that the two data sets were highly correlated ($P<0.001$). (Also see Supplementary Figure 1 for verification of microarray data by RT–PCR.)

With the use of RT–PCR, we then measured the amount of *AXIN2* mRNA in a larger number of samples (seven additional specimens of MSI$^+$ CRC, for a total of 17; 10 additional specimens of MSI$^-$ CRC, for a total of 20; three MSI$^+$ CRC cell lines; two MSI$^-$ CRC cell lines). The abundance of *AXIN2* transcripts in most of the MSI$^+$ CRC specimens and cell lines was reduced compared with that in the MSI$^-$ ones (Figure 2b); an *AXIN2*/*ACTB* transcript ratio of $<5\times10^{-4}$ was apparent in 13 of the 17 MSI$^+$ CRC specimens, but in only five of the 20 MSI$^-$ ones (Fisher's exact probability test, $P=0.003$). Importantly, a similar MSI-dependent suppression of *AXIN1* expression was not observed among these specimens ($P=0.31$) (data not shown).

Human *AXIN2* possesses a relatively large CpG island within its promoter region (nucleotide positions, chr17: 60986365–60987824). We therefore examined the methylation status of the CpG sites within this region by nucleotide sequencing after sodium bisulfite treatment. Extensive methylation of the CpG island in the *AXIN2* promoter was apparent in CRC specimens positive for MSI and for the loss of *AXIN2* expression (Figure 2c). The promoter region in the MSI$^+$ CRC cell line HCT116 (Wheeler *et al*., 1999) was also heavily methylated. The *MLH1* promoter in HCT116 cells is not methylated, but the coding sequence of the gene contains a mutation that results in MSI (Wheeler *et al*., 1999).

On the basis of these findings, we examined the methylation status of the *AXIN2* promoter in 37 clinical specimens and five cell lines by combined bisulfite restriction analysis (COBRA) (Xiong and Laird, 1997). CpG methylation was detected in five of the 17 MSI$^+$ specimens, but in none of the 20 MSI$^-$ specimens (Table 1; see Supplementary Table 2). Methylation of the *AXIN2* promoter was not detected in normal colon tissue obtained from the individuals with MSI$^+$ CRC (data not shown), suggesting that *AXIN2* methylation was a somatic event in these patients.

We then tested whether the amount of the encoded protein correlated with that of *AXIN2* mRNA in CRC specimens (Figure 2d). Immunohistochemical staining showed that AXIN2 was abundant in a specimen with a high mRNA content (ID308), but was present in much smaller amounts in two specimens with a low mRNA content (ID263, ID295). Although a large amount of *AXIN2* mRNA was not always associated with a large amount of protein, a small amount of mRNA was consistently associated with a small amount of protein (data not shown).

To examine directly whether epigenetic silencing of *AXIN2* is relevant to the change in the growth properties of CRC cells, we restored *AXIN2* expression, either by 5′-azacytidine treatment or by introduction of *AXIN2* cDNA, in an MSI$^+$ CRC cell line. 5′-Azacytidine inhibits *de novo* methylation of genomic DNA and thereby induces demethylation of the genome of proliferating cells (Christman, 2002). HCT116 cells were incubated for 3 days with various concentrations of 5′-azacytidine and were then subjected to COBRA for determination of the methylation status of the *AXIN2* promoter. Treatment with 5′-azacytidine reduced the level of methylation of the *AXIN2* promoter in a concentration-dependent manner (Figure 3a). This effect of 5′-azacytidine was accompanied by an increase in the amount of *AXIN2* mRNA in the cells (Figure 3b) as well as by the induction of cell death (Figure 3c).

Given that 5′-azacytidine likely affects the transcription of other genes in addition to that of *AXIN2*, the growth inhibitory effect observed in HCT116 cells might not have been attributable solely to the induction of *AXIN2* expression. To examine the direct effect of *AXIN2*, we introduced its cDNA into HCT116 cells by transfection. However, an introduction of *AXIN2* cDNA (even with the use of an inducible system) resulted in rapid cell death, and we could not establish stable transformants of cell lines with such expression constructs (data not shown). Therefore, we generated an amphotropic recombinant retrovirus that confers simultaneous expression of both an MYC epitope-tagged form of AXIN2 and mouse CD8. Human kidney 293 cells infected with this virus, but not those infected with a mock virus, expressed AXIN2 (Figure 3d). HCT116 cells were then infected with the virus and were subjected to affinity chromatography 48 h thereafter to isolate cells that express CD8. Given that CD8-expressing cells would be expected also to express AXIN2, this column purification step should result in rapid enrichment of AXIN2-expressing cells. The isolated cells indeed contained a substantial amount of *AXIN2* mRNA as revealed by RT–PCR (Figure 3e). The purified CD8$^+$ HCT116 cells were then cultured for 3 days to characterize their growth properties. Forced expression of AXIN2 resulted in marked inhibition of cell growth

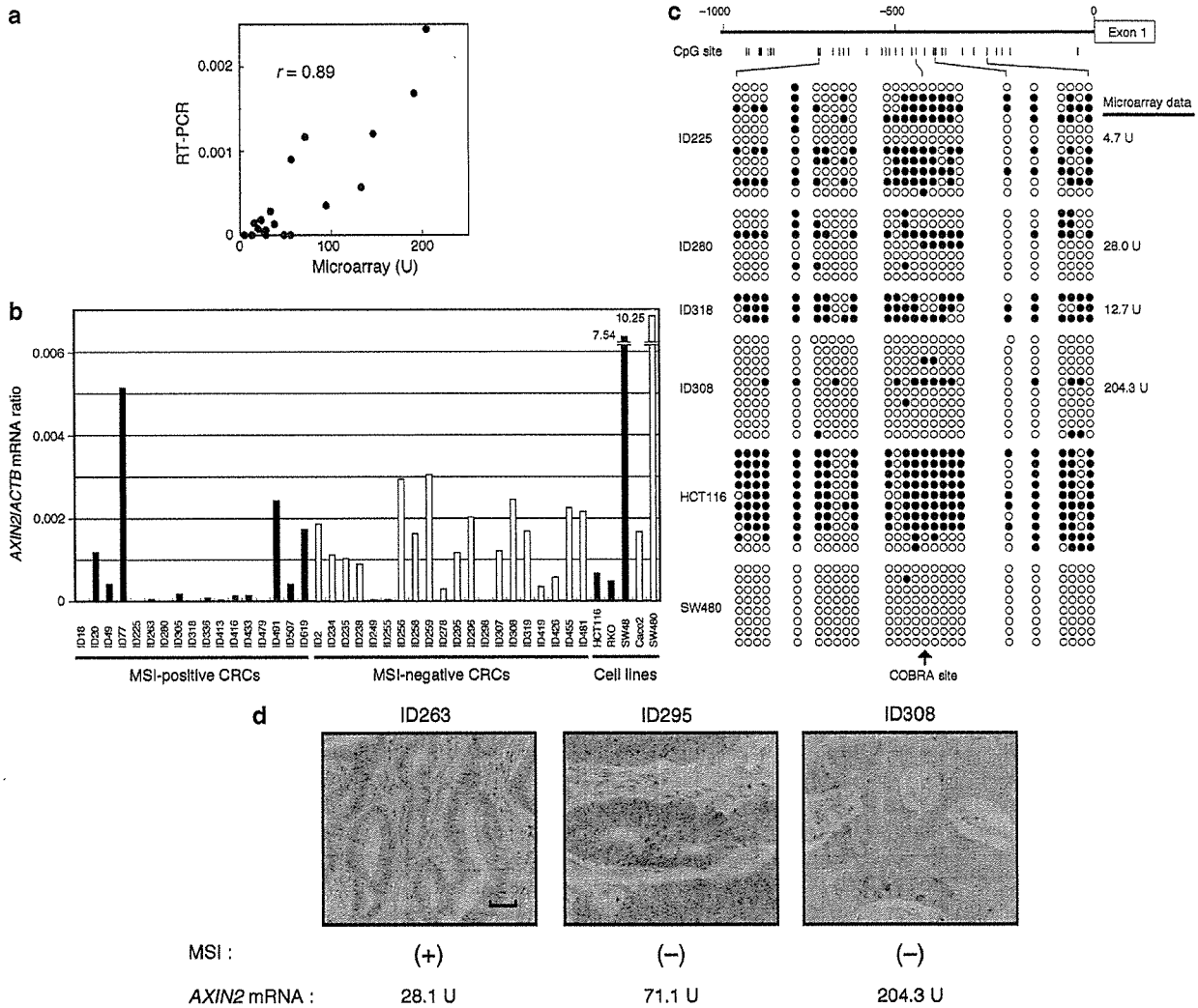

Figure 2 Suppression of *AXIN2* expression in CRCs positive for MSI. (**a**) Comparison of the abundance of *AXIN2* mRNA in study specimens as determined by microarray and RT–PCR analyses. For the latter, the amount of *AXIN2* mRNA was expressed relative to that of *ACTB* mRNA. Pearson's correlation coefficient (r) for the comparison is indicated. Portions of double-stranded cDNA were subjected to PCR with a QuantiTect SYBR Green PCR Kit (Qiagen). The amplification protocol comprised incubations at 94°C for 15 s, 63°C for 30 s, and 72°C for 60 s. Incorporation of the SYBR Green dye into PCR products was monitored in real time with an ABI PRISM 7700 sequence detection system (PE Applied Biosystems), thereby allowing determination of the threshold cycle (C_T) at which exponential amplification of products begins. The amount of target cDNAs relative to that of the β-actin (*ACTB*) cDNA was calculated from the C_T values with the use of Sequence Detector ver. 1.6.3 software (PE Applied Biosystems). The primers used for PCR amplification were 5′-CTGGCTCCAGAAGATCACAAAG-3′ and 5′-ATCTCCTCAAACACCGCTCCA-3′ for *AXIN2* and 5′-CCATCATGAAGTGTGACGTGG-3′ and 5′-GTCCGCCTAGAAGCATTTGCG-3′ for *ACTB*. (**b**) Comparison of the amount of *AXIN2* mRNA relative to that of *ACTB* mRNA (as determined by RT–PCR) between MSI$^+$ (closed bars) and MSI$^-$ (open bars) CRC specimens and cell lines. (**c**) Genomic DNA of the indicated clinical specimens and CRC cell lines was treated with sodium bisulfite (Koinuma *et al*., 2004), after which the *AXIN2* promoter region was amplified by PCR with the primers 5′-TTGTATATAGTTTA GYGGTTGGG-3′ and 5′-AAATCTAAACTCCCTACACACTT-3′. Closed and open circles indicate methylated and unmethylated CpG sites, respectively. The positions of the CpG sites are indicated at the top, the *Hha*I digestion site for COBRA is indicated by the arrow, and the microarray data for *AXIN2* expression are shown on the right. (**d**) Immunohistochemical analysis of the indicated clinical specimens with antibodies to AXIN2. The MSI status and the expression level of *AXIN2* determined by microarray analysis are indicated. Immunohistochemical analysis of AXIN2 expression was performed as described previously (Leung *et al*., 2002). Sections (5 μm) of formalin-fixed, paraffin-embedded tissue were mounted on Probe-On slides (Fisher Scientific), which were then incubated first for 1 h at room temperature with 1.5% normal horse serum and then overnight at 4°C with goat polyclonal antibodies to AXIN2 (Santa Cruz Biotechnology). Immune complexes were detected by the avidin–biotin–peroxidase method with 3,3′-diaminobenzidine as the chromogenic substrate (Vectastain ABC kit, Vector Laboratories). The sections were counterstained with hematoxylin. Scale bar, 50 μm.

(Figure 3f), indicating that silencing of *AXIN2* is indeed relevant to tumorigenesis. We also examined if the expression of *AXIN2* directly suppresses the WNT signaling pathway. For this purpose, we utilized a luciferase-based reporter plasmid (TOPflash) for the T-cell factor (TCF) activity, which is a direct target of

β-catenin (Korinek *et al.*, 1997). As shown in Figure 3g, a forced expression of *AXIN2* induced a marked suppression in the luciferase activity in HCT116 cells. On the other hand, *AXIN2* did not affect luciferase activity driven by a mutated, nonfunctional TCF-binding sites (FOPflash). These data clearly indicate that AXIN2 is involved in the WNT–APC–β-catenin pathway in CRCs.

We have demonstrated preferential transcriptional silencing of *AXIN2* in MSI$^+$ CRCs. Recently, mutations within exon 7 of the *AXIN2* gene have been reported in MSI$^+$ CRC specimens (Liu *et al.*, 2000; Wu *et al.*, 2001). We have thus analysed the nucleotide sequence of the *AXIN2* gene among our MSI$^+$ samples ($n=9$). Sequencing of the *AXIN2* exon 7 has revealed that only one patient (ID no. 263) carried a mutated *AXIN2* gene in one allele (data not shown). A deletion of a cytosine residue at the nucleotide position 2096 of the *AXIN2* cDNA (GenBank Accession Number, AF078165) led to a frame shift in the open-reading frame in this patient, introducing a premature termination codon in AXIN2 protein at the amino-acid position of 688. However, majority of the patients had intact *AXIN2* genes, indicating that silencing, but not mutation, of *AXIN2* is the main pathway to impede the *AXIN2* function.

The COBRA experiments revealed that the promoter region of *AXIN2* was extensively methylated in MSI$^+$ CRCs but not in MSI$^-$ CRCs. Although the difference in the frequency of *AXIN2* methylation between these two classes of tumor was significant (Fisher's exact probability test, $P=0.003$), the frequency for the MSI$^+$ specimens was still only 29% and therefore was not able to account for all the observed instances of suppression of *AXIN2* expression. We judged COBRA data as positive for methylation if $\geqslant 10\%$ of the PCR products were digested by *Hha*I. However, a small proportion ($<10\%$) of the PCR products was digested in the analysis of $\sim 50\%$ of MSI$^+$ CRC specimens (data not shown), indicating that alterations in the methylation status of the *AXIN2* promoter were more widespread. It is therefore possible that CpG sites other than that targeted by COBRA are more frequently methylated in MSI$^+$ CRCs and are more important for transcriptional regulation.

Similar promoter methylation has been recently described for other genes important for the WNT signaling pathway. The genes for secreted frizzled-related proteins are thus epigenetically silenced in MSI$^+$ CRCs, resulting in constitutive activation of the WNT pathway (Suzuki *et al.*, 2004). CpG sites within the *APC* promoter were also found to be frequently methylated in CRCs and other cancers (Esteller *et al.*, 2000; Zysman *et al.*, 2002). These data thus suggest that not only genetic mutations but also epigenetic silencing might play an important role in tumorigenesis mediated by activation of the WNT pathway.

Methylation of the *APC* promoter in endometrial cancer has been shown to occur preferentially in MSI$^+$ tumors (Zysman *et al.*, 2002). Despite the lack of an MSI-associated difference in the expression of *APC* in our CRC specimens (data not shown), the results of this previous study together with our present findings suggest the possibility that genes related to the WNT signaling pathway are targeted for methylation specifically in cancers with MSI. Our data further indicate that such methylation in MSI$^+$ cancers may be directly relevant to the mechanism of malignant transformation through epigenetic silencing of tumor suppressor genes. MSI$^+$ CRCs have been thought to arise through genetic events distinct from those that underlie MSI$^-$ cancers (Rajagopalan and Lengauer, 2004), which are frequently associated with aneuploidy and mutations in WNT pathway genes such as *APC* and *CTNNB1*. However, our data indicate that the molecular mechanisms for malignant transformation overlap between MSI$^+$ and MSI$^-$ CRCs.

Figure 3 Induction of cell death by restoration of *AXIN2* expression in a CRC cell line with a methylated *AXIN2* promoter. (**a**) HCT116 cells were incubated for 72 h with 0, 0.2, or 1 μM 5′-azacytidine and were then subjected to COBRA for determination of the methylation status of the *AXIN2* promoter (Xiong and Laird, 1997). Genomic DNA was denatured, incubated for 16 h at 55°C in 3.1 M sodium bisulfite, and then subjected to PCR with the primers in Figure 2c. The PCR products were then digested with the restriction endonuclease *Hha*I (Takara Bio), and the resulting DNA fragments were fractionated by polyacrylamide gel electrophoresis. The gel was stained with SYBR Green I (Takara Bio) and scanned with an LAS3000 imaging system (Fuji Film). Genomic fragments were determined to be positive for CpG methylation if $\geqslant 10\%$ of the PCR products were cleaved by the restriction endonuclease. Lane M, DNA size markers (50-bp ladder). (**b**) The cells from (**a**) were also subjected to RT–PCR analysis for determination of the amount of *AXIN2* mRNA relative to that of *ACTB* mRNA. (**c**) Cells treated as in (**a**) with 0, 0.2, 1, or 5 μM 5′-azacytidine were examined by light microscopy. Cell death was estimated by counting the remaining viable cells in each culture dish by the dye-exclusion method. Scale bar, 50 μm. (**d**) Human kidney 293 cells infected with either a mock virus or a recombinant virus encoding both MYC epitope-tagged AXIN2 and mouse CD8. A human cDNA for AXIN2 tagged at its NH_2-terminus with the MYC epitope sequence was ligated into the pMX-iresCD8 retroviral plasmid (Yamashita *et al.*, 2001) to yield pMX-AXIN2-MYC-iresCD8. The latter plasmid was introduced into BOSC23 cells together with pE-ampho and pGP packaging plasmids (Takara Bio) by transfection with the use of Lipofectamine (Invitrogen). The culture supernatant containing recombinant viruses was added to 293 cells with 4 μg/ml of polybrene (Sigma). Cells were then subjected to immunoprecipitation with the antibodies to MYC (9E10, Roche Diagnostics), and to immunoblot analysis with the same antibodies. (**e**) HCT116 cells infected with the viruses in (**d**) were subjected to affinity chromatography to isolate CD8$^+$ cells, which were then subjected to RT–PCR analysis for quantitation of *AXIN2* mRNA relative to the amount of *ACTB* mRNA. (**f**) The CD8$^+$ fractions in (**e**) were seeded at a density of 5×10^4 cells/dish and cultured for 72 h, after which the ratio of the final cell number to the initial value was determined. Data are means + s.d. of triplicate from a representative experiment. The *P*-value for the indicated comparison was determined by Student's *t* test. (**g**) HCT116 cells were seeded at a density of 2.5×10^6 cells/6 cm dish. After 24 h of incubation, the cells were transfected, with the use of Lipofectamine, with 2 μg of pMX-AXIN2-MYC-iresCD8 (AXIN2) or pMX-iresCD8 (Mock). For the reporter plasmids, 0.5 μg of pGL4 (Promega, Madison, WI, USA) plus either 0.5 μg of pTOPflash or 0.5 μg of pFOPflash (both from Upstate Biotechnology, Lake Placid, NY, USA) were added to the lipofection mix. The activity of *Photinus pyralis* luciferase was measured after 24 h of incubation with the use of the Dual-luciferase reporter assay system (Promega), and normalized on the basis of the activity of *Renilla reniformis* luciferase produced by pGL4. Data are shown as the mean value + s.d. of triplicate samples.

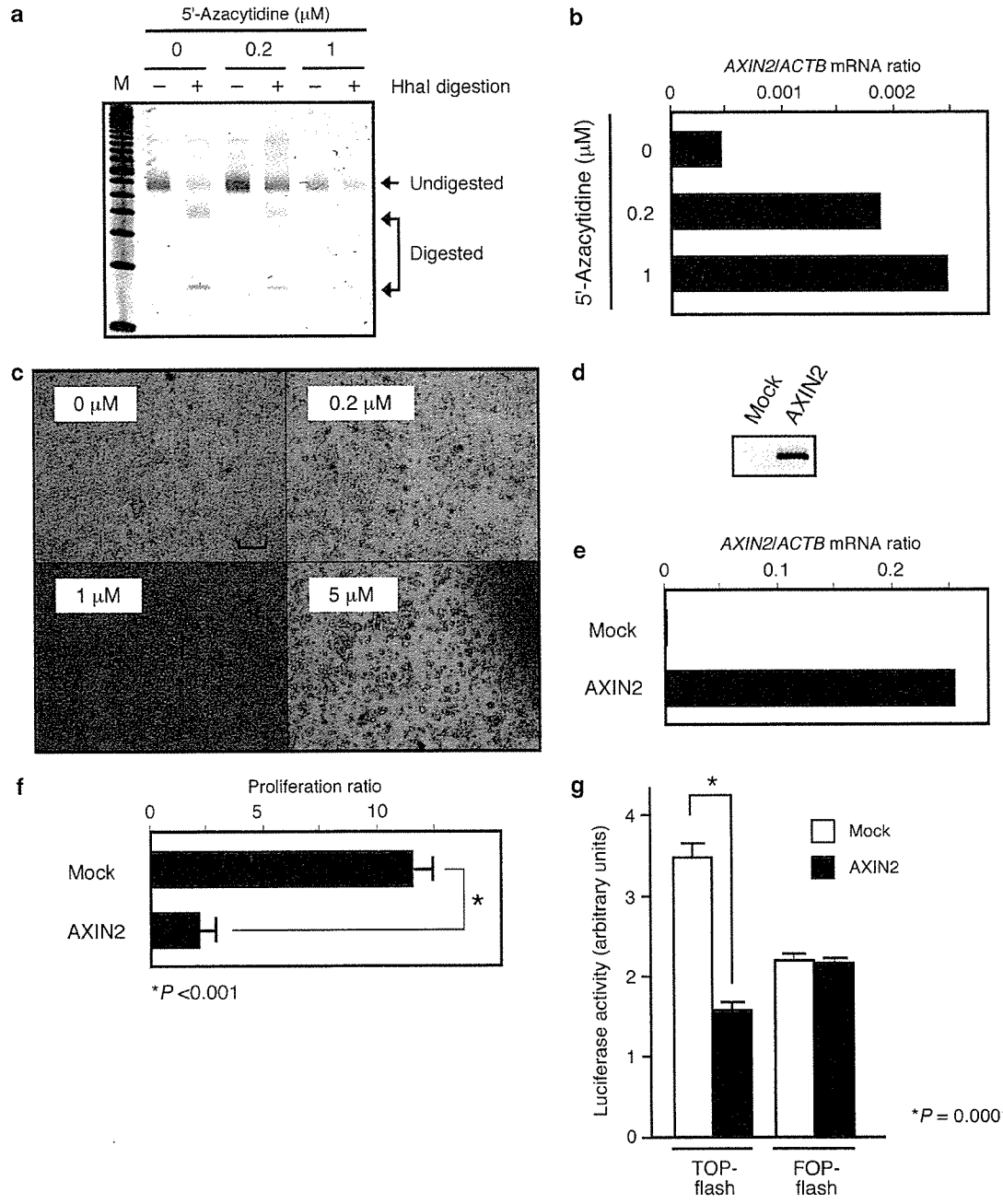

Acknowledgements

We thank M Toyota and SN Thibodeau for critical reading of the manuscript and helpful suggestions. This study was supported in part by a grant for Third-Term Comprehensive Control Research for Cancer from the Ministry of Health, Labor, and Welfare of Japan, and by a grant for 'High-Tech Research Center' Project for Private Universities: Matching Fund Subsidy (2002–2006) from the Ministry of Education, Culture, Sports, Science, and Technology of Japan.

References

Alon U, Barkai N, Notterman DA, Gish K, Ybarra S, Mack D *et al.* (1999). *Proc Natl Acad Sci USA* **96**: 6745–6750.

Behrens J, Jerchow BA, Wurtele M, Grimm J, Asbrand C, Wirtz R *et al.* (1998). *Science* **280**: 596–599.

Boland CR, Thibodeau SN, Hamilton SR, Sidransky D, Eshleman JR, Burt RW *et al.* (1998). *Cancer Res* **58**: 5248–5257.

Bronner CE, Baker SM, Morrison PT, Warren G, Smith LG, Lescoe MK *et al.* (1994). *Nature* **368**: 258–261.

Christman JK. (2002). *Oncogene* **21**: 5483–5495.
Cunningham JM, Christensen ER, Tester DJ, Kim CY, Roche PC, Burgart LJ *et al.* (1998). *Cancer Res* **58**: 3455–3460.
Esteller M, Sparks A, Toyota M, Sanchez-Cespedes M, Capella G, Peinado MA *et al.* (2000). *Cancer Res* **60**: 4366–4371.
Fellenberg K, Hauser NC, Brors B, Neutzner A, Hoheisel JD, Vingron M. (2001). *Proc Natl Acad Sci USA* **98**: 10781–10786.
Fishel R, Lescoe MK, Rao MR, Copeland NG, Jenkins NA, Garber J *et al.* (1993). *Cell* **75**: 1027–1038.
Ionov Y, Peinado MA, Malkhosyan S, Shibata D, Perucho M. (1993). *Nature* **363**: 558–561.
Issa JP. (2004). *Nat Rev Cancer* **4**: 988–993.
Kinzler KW, Vogelstein B. (1996). *Cell* **87**: 159–170.
Koinuma K, Shitoh K, Miyakura Y, Furukawa T, Yamashita Y, Ota J *et al.* (2004). *Int J Cancer* **108**: 237–242.
Korinek V, Barker N, Morin PJ, van Wichen D, de Weger R, Kinzler KW *et al.* (1997). *Science* **275**: 1784–1787.
Lengauer C, Kinzler KW, Vogelstein B. (1998). *Nature* **396**: 643–649.
Leung JY, Kolligs FT, Wu R, Zhai Y, Kuick R, Hanash S *et al.* (2002). *J Biol Chem* **277**: 21657–21665.
Liu W, Dong X, Mai M, Seelan RS, Taniguchi K, Krishnadath KK *et al.* (2000). *Nat Genet* **26**: 146–147.
Miyakura Y, Sugano K, Konishi F, Ichikawa A, Maekawa M, Shitoh K *et al.* (2001). *Gastroenterology* **121**: 1300–1309.
Narayan S, Roy D. (2003). *Mol Cancer* **2**: 41.
Ohki-Kaneda R, Ohashi J, Yamamoto K, Ueno S, Ota J, Choi YL *et al.* (2004). *Biochem Biophys Res Commun* **320**: 1328–1336.
Papadopoulos N, Nicolaides NC, Wei YF, Ruben SM, Carter KC, Rosen CA *et al.* (1994). *Science* **263**: 1625–1629.
Rajagopalan H, Lengauer C. (2004). *Nature* **432**: 338–341.
Rubinfeld B, Robbins P, El-Gamil M, Albert I, Porfiri E, Polakis P. (1997). *Science* **275**: 1790–1792.
Satoh S, Daigo Y, Furukawa Y, Kato T, Miwa N, Nishiwaki T *et al.* (2000). *Nat Genet* **24**: 245–250.
Smith G, Carey FA, Beattie J, Wilkie MJ, Lightfoot TJ, Coxhead J *et al.* (2002). *Proc Natl Acad Sci USA* **99**: 9433–9438.
Suzuki H, Watkins DN, Jair KW, Schuebel KE, Markowitz SD, Dong Chen W *et al.* (2004). *Nat Genet* **36**: 417–422.
Tolwinski NS, Wieschaus E. (2004). *Trends Genet* **20**: 177–181.
Toyota M, Ahuja N, Ohe-Toyota M, Herman JG, Baylin SB, Issa JP. (1999). *Proc Natl Acad Sci USA* **96**: 8681–8686.
Veigl ML, Kasturi L, Olechnowicz J, Ma AH, Lutterbaugh JD, Periyasamy S *et al.* (1998). *Proc Natl Acad Sci U S A* **95**: 8698–8702.
Wheeler JM, Beck NE, Kim HC, Tomlinson IP, Mortensen NJ, Bodmer WF. (1999). *Proc Natl Acad Sci USA* **96**: 10296–10301.
Wu R, Zhai Y, Fearon ER, Cho KR. (2001). *Cancer Res* **61**: 8247–8255.
Xiong Z, Laird PW. (1997). *Nucleic Acids Res* **25**: 2532–2534.
Yamashita Y, Kajigaya S, Yoshida K, Ueno S, Ota J, Ohmine K *et al.* (2001). *J Biol Chem* **276**: 39012–39020.
Zysman M, Saka A, Millar A, Knight J, Chapman W, Bapat B. (2002). *Cancer Res* **62**: 3663–3666.

Supplementary Information accompanies the paper on Oncogene website (http://www.nature.com/onc).